EurJIC
European Journal of Inorganic Chemistry

Review
doi.org/10.1002/ejic.202100410

Chemistry Europe
European Chemical Societies Publishing

Terminal Imido Complexes of the Groups 9–11: Electronic Structure and Developments in the Last Decade

Annette Grünwald,[a, b] S. S. Anjana,[a] and Dominik Munz*[a, b]

Dedicated to the legacy of Gregory L. Hillhouse.

We thank the Fonds der Chemischen Industrie (Liebig fellowship for D.M.), the German-American Fulbright Commission (Fulbright-Cottrell Award for D.M.) as well as the Bavarian Equal Opportunities Sponsorship – Realization of Equal Opportunities for Women in Research and Teaching (fellowship for A.G.) for financial support. We thank the RRZ Erlangen for computational resources.

1. Introduction

Multiple bonded complexes of late transition metals and their application in catalysis and group transfer chemistry are a thriving area of research. Especially complexes with highly covalent metal-ligand bonds, previously believed to be too reactive to be studied at room temperature, now find increasing attention. These complexes, which are in many cases only formally multiple bonded and often feature occupied *anti*-bonding molecular orbitals, show peculiar electronic structures. Hence, they activate strong C–H, C–C and C–F bonds, arguably paralleling heterogeneous catalysts, and some have been studied as single molecular magnets. In this review, we present a comprehensive, yet concise, update to Ray and coworkers' analysis on terminal oxo- and imido complexes of the groups 9 to 11 from 2013.[1] The chemistry of bridged complexes has been summarized elsewhere.[2]

This article is divided into subsections, starting with a very detailed discussion of nomenclature and the electronic structure of late transition metal imido complexes using computations. Readers with a dedicated interest in the coordination chemistry and synthesis are thus directly referred to the subsequent chapters. The multiple bonds with the group 9 elements will be summarized in section 3, whereas section 4 relates to the group 10 and section 5 to the group 11 elements. Section 6 addresses gas-phase and matrix studies of groups 9–12 terminal nitrido complexes. Beyond the aged, yet still leading, reviews on the electronic structure of multiple bonded complexes,[3] we further would like to draw the attention of the dedicated reader to recent summaries on terminal sulfido-[4] and oxo- complexes of the late 3*d* transition metals in the context of O–O bond formation and activation.[5] This is likewise the case for a perspective on functional group transfer with coordinatively unsaturated, charge-separated multiple bonded transition metal complexes ("vicinal zwitterions").[6]

2. Imido-, Imidyl- or Nitrene Ligand?

The electronic structure of formally *N*-, *O*-, *P*-, *S*-, *etc.*, π-donor multiple bonded complexes of the early transition metals is well established.[3a–c,7] This is even more true for carbene ligands, which are typically classified as nucleophilic, "Schrock-type" alkylidenes, electrophilic "Fischer-type" carbenes including ubiquitous *N*-heterocyclic carbene (NHC) ligands, or carbene radicals.[8] However, the electronic structure of formally *N*-, *O*-, *P*-, multiple bonded complexes of the late transition metals is less clear,[3e,9] though analogies with carbene chemistry have been pointed out.[10] The nomenclature used for, in particular, imido complexes easily leaves the reader puzzled. For instance, Hillhouse' covalently bonded, d^8 configured, linear (NHC) Ni=NAr complex with a triplet ground state (*vide infra*) was referred to as a "nickel imido complex that engages in nitrene-group transfer".[11] Contrarily, the related (dtbpe)Ni=NAr (dtpbe: 1,2-bis(di-*tert*-butylphosphino)ethane) complex, which shows a singlet ground state, was referred to by the same group as a "nickel nitrene" in sight of its "nitrene transfer reactivity".[12] Indeed, basic or rather nucleophilic complexes are often associated with an "imido-" ligand, whereas open-shell reactivity and electrophilicity are commonly connected with a "nitrenoid-" (in the sense of "nitrene-like"), "nitrene-" or "imidyl-" electronic structure of the ligand. Hence, the terms "imido", "imide", "nitrene" "nitrenoid", "imidyl" and "iminyl" are frequently used to describe complexes with an equivalent electronic structure. Similar ambiguity has been outlined for naming carbenes, alkylidenes, carbenoids and carbene radicals.[13] We hence wish to clarify the connection between nomenclature and electronic structure including the terms

[a] *A. Grünwald, Dr. S. S. Anjana, Prof. D. Munz*
Inorganic Chemistry: Coordination Chemistry
Saarland University
Campus Geb. C4.1, 66123 Saarbücken,
Germany
E-mail: dominik.munz@uni-saarland.de
https://www.uni-saarland.de/lehrstuhl/munz.html
[b] *A. Grünwald, Prof. D. Munz*
Inorganic and General Chemistry
Friedrich-Alexander Universität (FAU) Erlangen-Nürnberg
Egerlandstr. 1, 91058 Erlangen, Germany

Review
doi.org/10.1002/ejic.202100410

"imido/imide", "iminyl/imidyl", "nitrene", "nitrenoid" and "nitrene radical".

A nitrene is a monosubstituted nitrogen atom with an electron sextet (Figure 1, left). It may assume a triplet ground state, as is the case for imidogen (NH), or alternatively may be a singlet as found for acylnitrenes.[14] Azanidyl or imidyl relate to the monoanionic, seven-electron radical congeners, as is also the case for iminyl radicals. The latter term emphasizes a formal double bond to an adjacent sp^2 configured carbon atom (Figure 1, middle).[15]

Azandiides (or imides) are the dianionic congeners with an electron octet (Figure 1, right). Classically, RN ligands, formally (*sic!*) double bonded to metals, are referred to as "imido" ligands.[16] Imido ligands of the early and thus electropositive transition metals are understood by their bisanionic electronic structure RN^{2-}. In these complexes, the ligands can be up to triply bonded due to the interaction of the *p*(z) (*sp* hybrid, respectively) orbital (σ-bond) as well as the *p*(x) and *p*(y) orbitals (π-bond) with the metal's vacant valence *d*-orbitals of appropriate symmetry. In case of high triple-bond character, they are electrophilic; for lower bond orders, nucleophilic reactivity dominates in the absence of open-shell character. Since the ligand centered orbitals in these early transition metal complexes are comparably low in energy, they are well separated from the *d*-orbitals (Figure 2A). Accordingly, the electronic structure is well approximated by common ligand-field splitting diagrams and an ionic donor-acceptor picture, respectively.

However, the energies of the valence *d*-orbitals decrease when moving to the late transition metals (Figure 2B); the same is true when moving from the 3*d* to the 4*d* or 5*d* elements of the late transition metals[17] or for high-valent complexes of the group 8 and 9 metals. This renders the bonds with the ligands increasingly covalent and reduces the formal bond order due to the population of *anti*-bonding molecular orbitals. Consequently, a myriad of resonance structures may be of relevance for such imido complexes.[18] Note that, although commonly found in the literature, simplified ligand field splitting diagrams

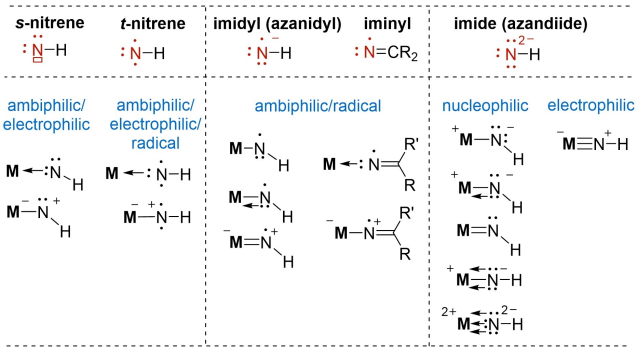

Figure 1. Resonance structures and nomenclature of RN ligands.

are only moderately illustrative for the underlying electronic structures.

Eventually, the *p*-orbitals of the *N*-donor ligands will end up higher in energy than the metal's occupied *d*-orbitals (Figure 2C), giving rise to an orbital inversion or an "inverted ligand field".[19] This may lead to a nitrene-ligand electronic structure, or, in case of paramagnetic complexes, to an imidyl ligand, *i.e.* a nitrogen ligand centered radical in first approximation, isoelectronic with the radical oxyl ligand.[20] However, the assignment of a simplified electronic structure to a covalently bound ligand is fairly arbitrary and depends strongly on the chosen computational method.

Methods relying on a selected active space of orbitals for a number of electrons ("complete active space SCF", CASSCF) usually show a strong dependence on the choice of the active space. In case of such multiconfigurational calculations, configurations associated with "nitrene", "imido" and "imidyl" character may contribute considerably to the overall electronic structure (*vide infra*), which further complicates the assignment of an approximate Lewis structure.

Overall, we conclude that "imido" ligand appears formally to be a good designation for any of the above discussed electronic

Annette Grünwald was undergraduate student at Leipzig University (B.Sc.: 2014) and obtained her M.Sc. degree at FAU Erlangen-Nürnberg under the tutelage of N. Burzlaff in bioinorganic chemistry in 2016. In 2017, she initiated and subsequently established the palladium chemistry in the young group.

Anjana received her M.Sc. in Chemistry from Kerala University in 2010. She then moved to IIT Madras for doctoral research in bioinorganic chemistry under the supervision of N. N. Murthy and E. Prasad and completed her PhD in 2017. After a stint at IIT Bombay as a postdoctoral researcher in the area of transition metal assisted C–H functionalization with G. K. Lahiri and D. Maiti, she joined the Munz group at Saarland University.

Dominik Munz studied chemistry and chemical engineering at TU Dresden and ENSC Rennes. He obtained his diploma (2009) and doctoral degree (2013) for work with T. Strassner in Physical Organic Chemistry (TU Dresden). He performed postdoctoral work with T. B. Gunnoe (University of Virginia) and G. Bertrand (UC San Diego) in the areas of late transition metal catalysis and p-block chemistry. Prior to his current position at Saarland University, he was junior group leader ("habilitand") associated with the chair of K. Meyer at FAU Erlangen-Nürnberg (2016–2020). His scientific interests comprise functional group transfer and the activation of strong bonds, redox catalysis, and photochemistry with biradicals, zwitterions, or more generally organic electronic materials.

Review
doi.org/10.1002/ejic.202100410

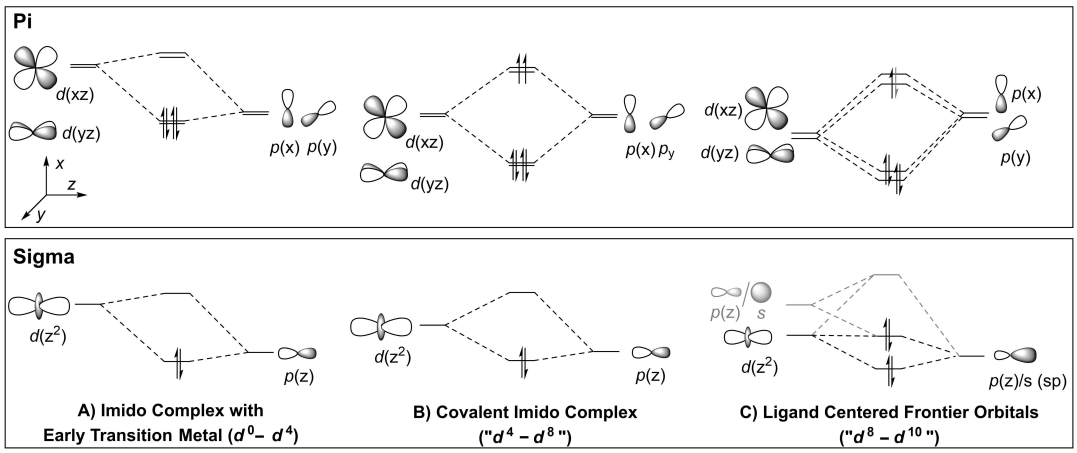

Figure 2. Idealized orbital interactions in transition metal imido complexes. Non-bonding $d(x^2\text{-}y^2)$ and $d(xy)$ orbitals are omitted for clarity.

structures. Additionally, "imide" seems useful to emphasize nucleophilic reactivity. Further, we suggest not to use "nitrenoid", since it is, in analogy to the misleading usage of the term "carbenoid",[13] not clearly defined. The term "iminyl" should be used with caution since the (formal) double bond to an α-carbon atom ("imine") could be confused with the (formal) double bond to the metal. We discourage the term "nitrene" to generally refer to open-shell reactivity, but instead recommend using it deliberately for an electronic structure with two ligand centered radicals ("triplet-nitrene ligand"). Eventually, we would like to highlight that in cases of high covalency, the assignment of these simplified electronic structures becomes arbitrary to quite some extent.[21]

According to simplified ligand field considerations, some formally multiple bonded late transition complexes should have a bond order of zero. However, the mixing of metal-based orbitals reduces their *anti*-bonding character. For instance, mixing of a formally occupied $3d(z^2)$ orbital with the 4*s* orbital reduces the extension of the axial lobes in the *z*-direction (Figure 3, left), whereas mixing with the 4*p*(z) orbital polarizes the axial lobes towards one direction (Figure 3, right).

It is important to note that the polarization of *d*-orbitals is not a computational artefact and symmetry allowed mixing is, of course, well founded in molecular orbital- (MO-) and group theory.[22] For instance, *s*/*d* mixing is responsible for unusual structures, defying Valence Shell Electron Pair Repulsion (VSEPR)

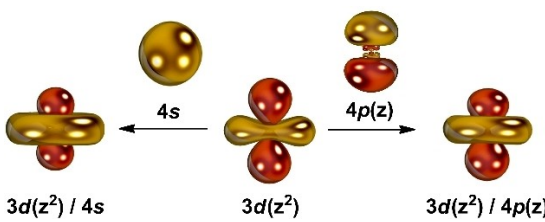

Figure 3. Mixing of an occupied $d(z^2)$ orbital with a vacant *s* or vacant *p*(z) orbital may attenuate its *anti*-bonding character.

theory of d^0 configured metal complexes.[23] Further experimental indication for such hybridization comes from K-edge 1 *s*→3*d* X-Ray absorption spectroscopy (XAS)[24] of terminal iron(IV) nitrides.[25] Similarly, non-bonding *d* -orbitals may mix, as was shown by Electron Paramagnetic Resonance (EPR) and Electron Nuclear Double Resonance (ENDOR) spectroscopies for Smith's iron(V) nitrido complex.[26] The interplay of Jahn-Teller distortion and spin-orbit coupling induced orbital mixing has been also investigated in detail for a handful of iron complexes in threefold symmetry.[27]

In the following sections, we will present a detailed discussion on the electronic structures sketched above in Figure 2, using representative early and late transition metal imido complexes from the literature.

1) Niobium(V): Coordinative Triple Bond: The yellow d^0 configured tris-amido imido niobium complex **1** serves as an example for an early transition metal imido complex in pseudo-tetrahedral coordination with a metal-imido triple bond (Figure 4, left).[28] The σ-interaction can be understood as a coordinative interaction, whereas the two π-bonds show significant covalency (ligand : metal = 8 : 2). The HOMO-1 is stabilized (in reference to the HOMO) due to significant mixing with the π-system of the phenyl substituent. This complex shows a large singlet-triplet gap $\Delta E^{s/t}$ exceeding 3 eV and the weight of the lead configuration in a CASSCF calculation amounts to 70 %, where the remaining configurations relate essentially to π–π* excitations within the imido substituent.
2) Palladium(II): Strongly Covalent, Zwitterionic Single Bond: An example of high covalency is the diamagnetic terminal sulfonimido complex **2**, supported by a functionalized cyclic (alkyl)(amino) carbene ligand (^{fun}CAAC; see also Figure 27 below).[29] According to simplified ligand-field considerations, this imido complex should feature a bond order of zero and hence be thermodynamically unstable. However, not only the bonds with the imido ligand, but also the σ- as well as π-bonding interactions with the ancillary carbene- and imine- ligand are highly covalent,

Review
doi.org/10.1002/ejic.202100410

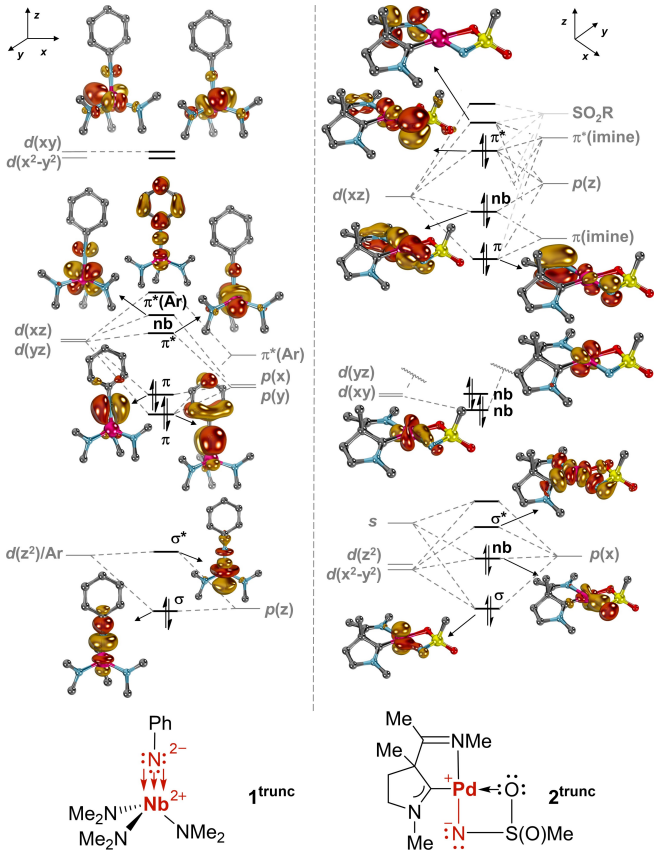

Figure 4. Molecular orbitals in truncated niobium(V)- [left; sa-CAS(6,9); $\mathbf{1}^{trunc}$] and truncated palladium(II)-imido [right; sa-CAS(18,12); $\mathbf{2}^{trunc}$] model complexes. Hydrogen atoms are omitted for clarity.

and further mixing between the 4*d* and 5*s* orbital is computationally obtained (Figure 4, right). This renders the assignment of a formal oxidation state challenging, yet a formal d^8 configuration seems to describe the electronic structure of this compound best. Also, constructing a concise molecular orbital diagram reveals a fairly complicated mixing pattern. It was experimentally shown that the interaction with the labile oxygen-donor site is comparably weak, which is also corroborated by few orbital admixtures related to the imido- or metal-centered molecular orbitals as well as the strong positive partial charge at the metal.[29] The HOMO relates to the imido-ligand centered (ligand:metal = 0.7:0.3), *anti*-bonding combination of the π-bond with the metal, combined with some overlap with the π-system of the imino ligand in *para*-position (0.04) as well as (negative) hyperconjugation with the sulfonyl group (0.06). This mixing with orbitals of higher energy weakens the *anti*-bonding character of the HOMO, which overall results in a (weakly) bonding interaction with the imido's *p*(z) orbital. It is interesting to note that such mixing with the π-acidic imino ligand in *para*-position was also suggested by Limberg to be important for the stabilization of late transition metal terminal oxo complexes.[30] A bonding σ-orbital forms through the overlap of the metal's $d(z^2)$ with the *p*(x) orbital of the imido ligand. The *anti*-bonding character of the related σ*-orbital is attenuated through mixing with the 5*s* orbital of the palladium ion. Further minor bonding interactions are obtained through lateral interaction (the O-Pd-N angle is only 73°) of the imido nitrogen centered *p*(x) orbitals with the *d*(xy) orbital. Eventually, the computations corroborate the presence of a σ-bond with the sulfur atom involving the *p*(y) orbital of the nitrogen atom, in combination with another lone pair at the imido nitrogen atom residing in the 2*s* orbital. Overall, all orbital interactions give rise to a single bond between the metal and the imido ligand and strong vicinal zwitterionic character as has been discussed[6,31] in the context of Frustrated Lewis Pair (FLP) type chemistry. Negligible open-shell character is corroborated by the large singlet-triplet gap ($\Delta E^{s/t} = 2.6$ eV) and the high weight of 0.82 for the lead closed-shell configuration $c^{"(2,0)"}$ in the CASSCF calculations, whereas the diradical resonance structure $c^{"(1,1)"}$ accounts only for 0.05 (Figure 5, left). This stands in stark contrast to Hillhouse's bisphosphine- ($\mathbf{3}^{trunc}$; Figure 5 middle) and di(NHC) ($\mathbf{4}^{trunc}$; Figure 5 right) supported imido complexes.[32] For $\mathbf{3}^{trunc}$ and $\mathbf{4}^{trunc}$, at the same level of theory, the radical configurations $c^{"(1,1)"}$ relating to the (excited) triplet state are predicted to mix considerably with the lead closed-shell configuration $c^{"(2,0)"}$ of the ground state ($\mathbf{3}^{trunc}$:0.47:0.46, $\Delta E^{s/t} = 0.8$ eV; $\mathbf{4}^{trunc}$:0.79:0.15; $\Delta E^{s/t} = 1.3$ eV).[33] Thus, the imido ligands in these complexes share high to moderate triplet-nitrene character. In any case, **2** also features weak electrophilic properties as proven by the formation of iminophosphoranes in reaction with phosphines (*vide infra*).

3) Cobalt(II): Covalent Multiple Bond, Metal-Centered Radical: The trisphosphine-coordinated cobalt complex **5** (see also Scheme 6 below) illustrates the electronic structure of an imido ligand bonded to an open-shell metal ion of the late transition metals (Figure 6, left).[35] The vacant $3d(z^2)$ orbital is *anti*-bonding. It hence admixes the 4*s* as well as to a much minor extent the 4*p*(z) orbital, which mitigate its *anti*-bonding character (*d*:*s*:*p* = 7:2.9:0.1). Of the two π-bonds, the one without conjugation with the phenyl ring is very covalent (ligand:metal = 6:4). In absence of conjugation with the phenyl ring, the *anti*-bonding orbital is higher in energy and hence vacant. The other π-bond is margin-

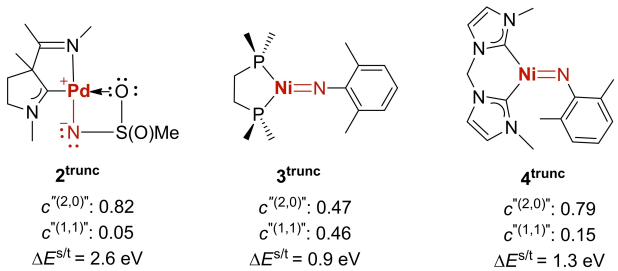

Figure 5. CASSCF/NEVPT2 calculations indicate that palladium complex $\mathbf{2}^{trunc}$ [sa-CAS(18,12)] is a vicinal zwitterion ion, whereas the nickel complexes $\mathbf{3}^{trunc}$ [sa-CAS(16,12)] and $\mathbf{4}^{trunc}$ [sa-CAS(16,12)] share triplet-nitrene character.[34]

Review
doi.org/10.1002/ejic.202100410

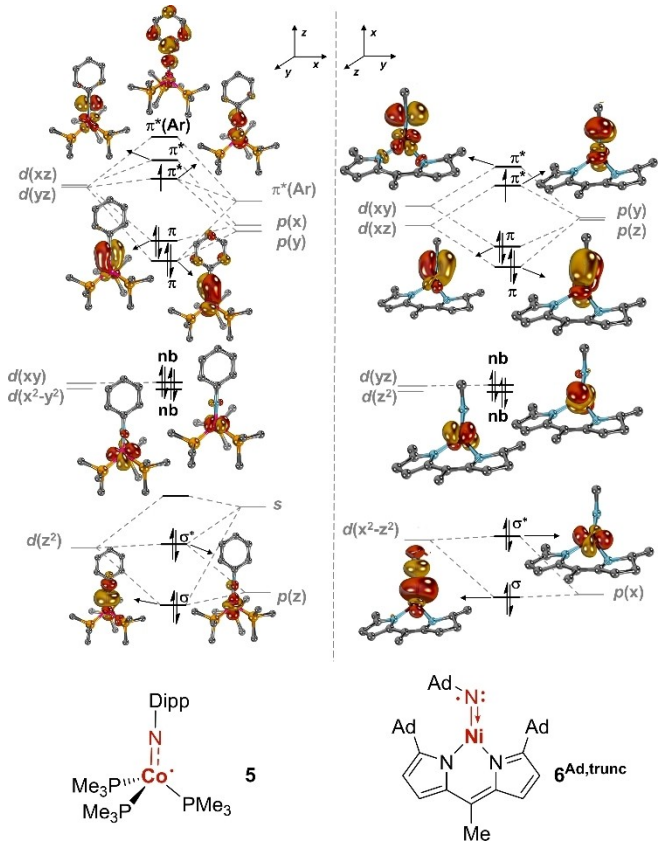

Figure 6. Molecular orbitals in cobalt(II) imido [left; CAS(13,9); **5**] and nickel (II) imidyl [right; CAS(13,8); $\mathbf{6}^{Ad,trunc}$] model complexes. Hydrogen atoms in **5**, as well as adamantyl substituents in $\mathbf{6}^{Ad,trunc}$ are omitted for clarity.

ally covalent (ligand : metal = 9 : 1), stabilized through interaction with the π-system of the aryl substituent, and the *anti*-bonding, metal-centered combination of predominantly *d*(yz) character is populated by one electron. Overall, this electronic structure is consistent with a d^7 configured cobalt(II) ion. Yet, this compound shares small imidyl character in its ground state as corroborated by a calculated population of 0.3 e^- of the π* orbital, which translates into a Löwdin spin density of −0.1 a.u. at the imido nitrogen atom.

4) Nickel Imidyl Complex: Betley and colleagues reported mesityl- and adamantyl (Figure 6, right) imido complexes of nickel, supported by a dipyrrinato ligand ($\mathbf{6}^{Mes}$ and $\mathbf{6}^{Ad}$; see also Figure 22 below).[36] Compound $\mathbf{6}^{Ad}$ can be understood as nickel imidyl complex and features an unpaired electron at the nitrogen ligand. The two π-bonding interactions in $\mathbf{6}^{Ad,trunc}$ reveal high covalency. The π-orbital involving the *d*(xz) orbital is rather metal-centered (ligand : metal = 4 : 6), and the *anti*-bonding combination, occupied by one electron, is accordingly ligand centered (ligand : metal = 6 : 4). The doubly occupied π-orbital relating to the *d*(yz) orbital is as well ligand centered (ligand : metal = 6 : 4), which overall leads to a formal d^8 electron configuration of the nickel ion. Contrarily, the electronic structure of $\mathbf{6}^{Mes}$, which shows predominant spin-density at the metal, was suggested to lean rather towards the nickel(III) side.

5) Nickel Triplet-Nitrene Complex: Hillhouse' formally d^8 configured (NHC)Ni(NAr) imido complex **8**[11] is the seminal example for a covalently bonded imido ligand with strong nitrene character, *viz.* a nickel supported triplet-nitrene (Figure 7, left). The two π- as well as two π*-orbitals are populated by overall six electrons giving rise to an $S = 1$ ground state. These orbitals are essentially evenly distributed between the metal and imido ligand (ligand : metal = 5 : 5), thus suggesting strong triplet-nitrene character for the imido ligand. Also here, the nitrene is stabilized through conjugation with the aryl substituent. Of further note, the $3d(z^2)$ orbital shows admixture of *s* character ($s : d = 3 : 7$), which attenuates its *anti*-bonding nature. In case of Betley's copper supported triplet-nitrene **7** (*cf.* Figure 27), an analogous electronic structure was computed. Yet, even stronger ligand-centered character of the two *anti*-bonding molecular orbitals of π-symmetry (ligand : metal = 6 : 4) is found for the latter, thus giving rise to a "genuine" triplet-nitrene ligand.[37]

6) Platina Triplet-Nitrene: Schneider's platinum nitride complex **9** is a *bona fide* platina triplet-nitrene (Figure 7, right).[38] Both π*-orbitals are singly occupied and clearly

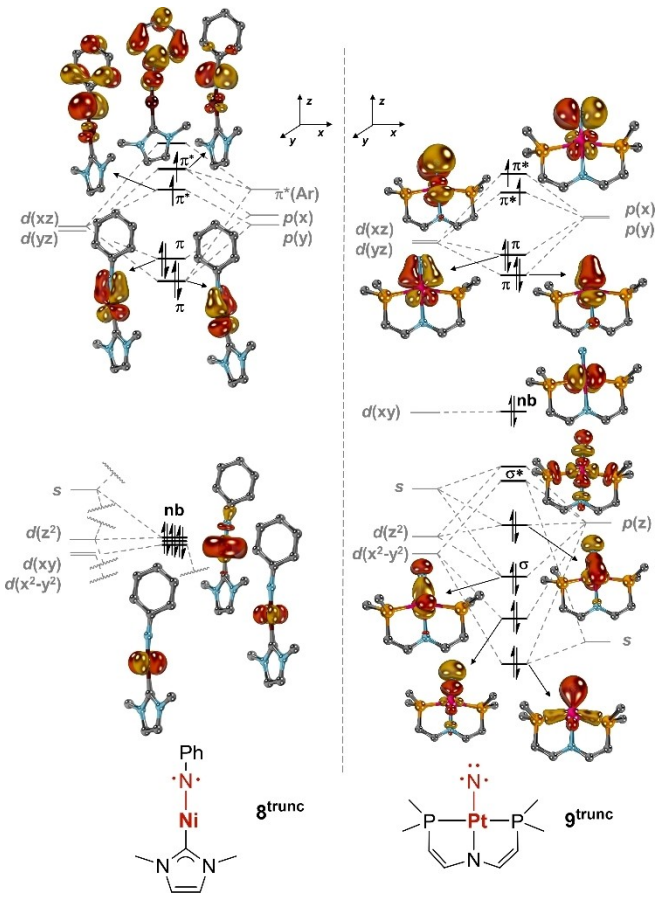

Figure 7. Molecular orbitals in nickel triplet-nitrene [left; CAS(12,8); $\mathbf{8}^{trunc}$] and planar platina triplet-nitrene [right; sa-CAS(18,12); $\mathbf{9}^{trunc}$] model complexes. Hydrogen atoms are omitted for clarity.

ligand centered (ligand : metal = 8 : 2), whereas the σ-interaction is considerably covalent. The *anti*-bonding combination, which relates mostly to the $5d(z^2)$ orbital, combines with the nitrene's 6*p*(z) orbital and shows large (20%) admixture of the metal's 6*s* orbital.

7) Ylidic Stabilization: It is well known that formally cationic substituents such as imidazolium- groups stabilize anions through mesomeric effects. Prominent examples for this effect are the *N*-heterocyclic imines (Figure 8). Thus, these scaffolds have also been applied as "masked" imido-ligands with comparatively tamed nucleophilicity. Note that the group 14 congeners, namely *N*-heterocyclic olefins, have received considerable attention as well.[39] Although no open-shell derivatives have been isolated to the best of our knowledge, their electronic structure seems to be similar to the above-discussed iminyl complexes. Since the chemistry of these complexes has been comprehensively covered elsewhere, we refer the interested reader to these reviews.[40]

8) Mesomeric Effects in Arylimido Complexes: As outlined above and emphasized by the designation "iminyl", imido complexes benefit from conjugative stabilization with aryl substituents. In the case of nucleophilic, diamagnetic imido complexes, the aryl group delocalizes the negative partial charge, whereas spin density is distributed in case of iminyl/imidyl or nitrene ligands. The structural parameters of the arene substituents as obtained by single crystal X-ray diffraction (SC-XRD) analysis allow to approximate the degree of delocalization through the shortening of the *N*–C^{ipso} and elongation of the C^{ipso}–C^{ortho} bonds (Figure 9).

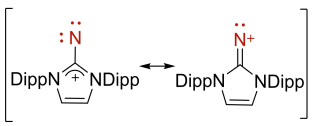

Figure 8. Ylidic imido- ligands

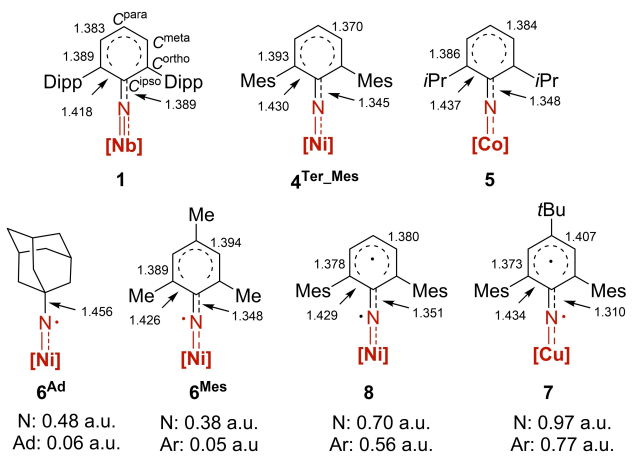

Figure 9. Averaged bond lengths in the solid state (values are given in [Å]) and calculated (PBE–D3/def2-SVP) Löwdin spin densities in open-shell arylimido complexes (bottom).

For instance, the niobium complex **1** shows a much smaller *N*–C^{ipso} bond length (*N*–C^{ipso} = 1.389 Å) than the nickel imidyl complex $\mathbf{6^{Ad}}$ (*N*–C^{ipso} = 1.456 Å); the *N*–C^{ipso} bonds in the late transition metal imido complexes $\mathbf{4^{Ter\_Mes}}$ (*N*–C^{ipso} = 1.345 Å) and **5** (*N*–C^{ipso} = 1.348 Å) are even shorter. This is likewise the case for the imidyl complex $\mathbf{6^{Mes}}$ (*N*–C^{ips} = 1.348 Å) as well as the nitrene complexes **8** (*N*–C^{ipso} = 1.351 Å) and particularly **7** (*N*–C^{ipso} = 1.310 Å). Among the latter three complexes, only little spin density is localized at the aryl substituent in $\mathbf{6^{Mes}}$ (5%), whereas high spin delocalization is calculated for **8** (56%) and **7** (77%).

9) Metal–Nitrogen Bond Lengths: Triply bonded (*vide supra*) niobium(V) imido complex **1** has a Nb–N bond length of 1.794(2) Å (Figure 10),[28] which is longer than that found for the 3*d* vanadium complex **10** (1.638(4) Å).[41] The Co–N bond of neutral terminal cobalt(II) imido complex **5** measures 1.7089(15) Å,[35] whereas the one of dicoordinate $\mathbf{11^{dmp}}$ is shorter with 1.691(6) Å.[42] Formal cobalt(III) imido complexes tentatively exhibit shorter Co–N bonds as illustrated by $\mathbf{12^{Tol}}$ (1.6668(18) Å)[43], **13** (1.658(2) Å)[49c] and **14** (1.632(3) Å)[44], whereas the Co–N bond length in anionic cobalt(III) complex **15** (1.7067(12) Å), which shares imidyl character, is of similar magnitude.[56] Importantly, the oxidation of $\mathbf{16^{+}}$ (1.649(1) Å) to $\mathbf{16^{2+}}$ (1.702(3) Å) resulted in considerable elongation of the Co–N bond.[45] This observation, contradicting the common shortening of metal–ligand bonds upon oxidation, was computationally rationalized by enhanced imidyl- and even partial nitrene character for $\mathbf{16^{2+}}$. Indeed, cobalt(IV)- and cobalt(V) diimido complexes **17** and $\mathbf{17^{+}}$ feature shorter Co–N bonds of 1.665(3) and 1.640(3) Å, respectively.[59] Moving down the group to tetracoordinated 4*d* rhodium(III) complex **18**, which is isostructural with $\mathbf{12^{Tol}}$, reveals a larger Rh–N distance of 1.780(2) Å.[72] This effect is enhanced for the hexacoordinated nitrene complex **19** (2.303(4) Å).[78,79] Moving to the 5*d* element iridium reveals arguably similar bond lengths as found for rhodium. The tetracoordinated iridium(III) imidyl complex **20** shows an Ir–N bond length of 1.805(2), which also here further elongates upon oxidation to $\mathbf{20^{+}}$ (1.868(2) Å) due to enhanced nitrene character.[46] Tricoordinated nickel(II) imido complexes such as $\mathbf{3^{Ad}}$ (1.657(5) Å)[47] and imidyl complex $\mathbf{6^{Ad}}$ (1.642(7) Å)[36] show Ni–N bonds in the range of 1.64–1.70 Å.[32a,b] The strongly bent nickel(II) imido $\mathbf{4^{Ter\_Mes}}$ with unusual strong closed-shell character exhibits a significantly longer Ni–N bond (1.732(3) Å).[89] The Pd^{II} imido complex **2** features a Pd–N single bond (2.0423(19) Å) due to hyperconjugation of the imide ligand with the electron-withdrawing tosyl moiety.[29] In line with its nitrene electronic structure, copper complex **7** exhibits in comparison to the cobalt- and nickel complexes a long copper–nitrogen bond of 1.759(2) Å.[37]

10) Imido Complexes – Bent or Linear? Generally, imido ligands are linear except the nitrogen atom bears considerable lone-pair- or mono-radical character (Figure 11). Thus, triply bonded imido ligands of complexes with a low *d*-electron number as well as nitrene ligands are linear or close to

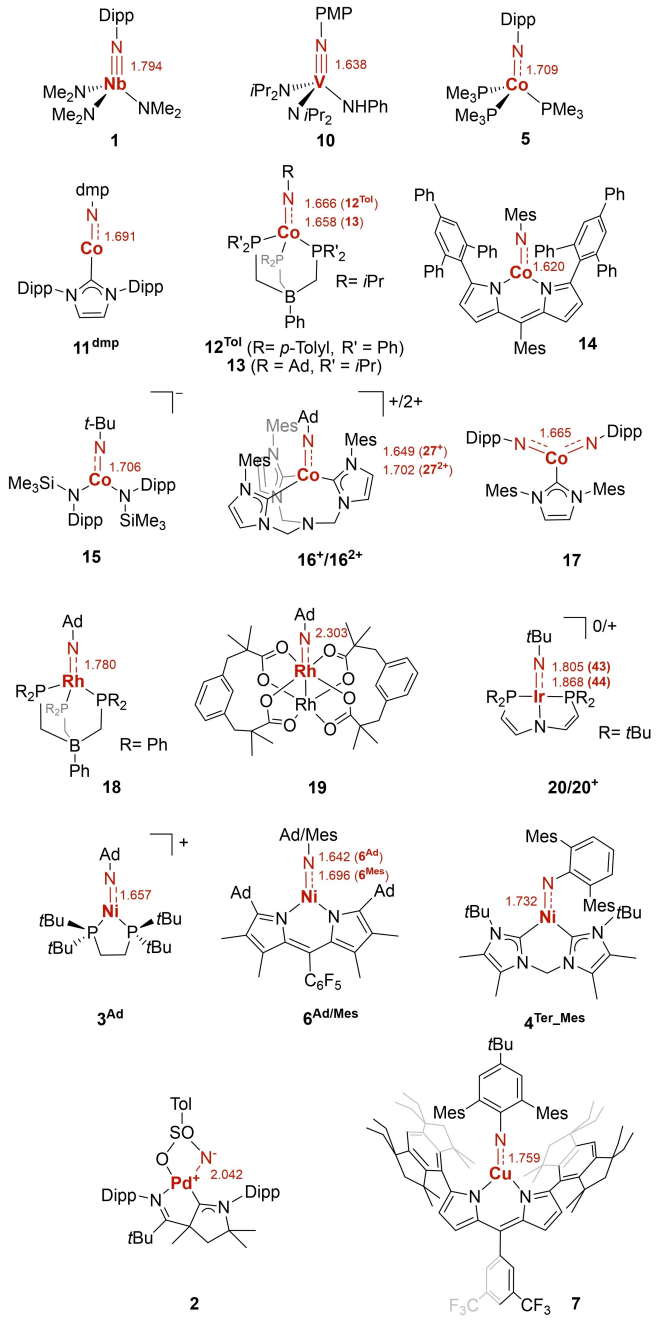

Figure 10. Metal–imido bond lengths (values are given in [Å]) of selected examples in the solid state.

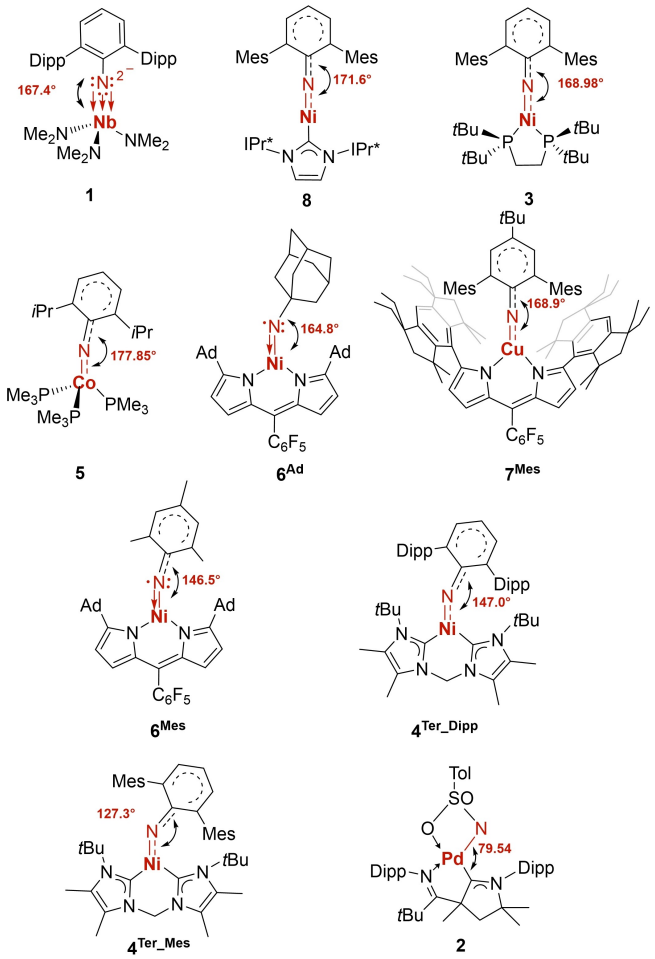

Figure 11. Angles of imido linkages of selected examples in the solid state.

linearity, respectively. Examples are the complexes **1** (M-N-R = 167.4(2)°)[28] and **8** (M-N-R = 171.6(3)°)[11]. Also the cobalt imido complex **5**, where the bonding interaction is due to π-interactions only, features a close-to-linear imido linkage (M-N-R = 177.85(14)°).[35] The same is true for nickel complex **3**, where the singlet ground state shows strong admixture of open-shell excited states (*viz.* nitrene character).[32b] The picture is less clear for imidyl complexes. For instance, $\mathbf{6}^{Ad}$ (M-N-R = 164.8(17)°)[36] and $\mathbf{7}^{Mes}$ ((M-N-R = 168.9(1)°)[37] are at best moderately bent. On the contrary, the linkage in complex $\mathbf{6}^{Mes}$, where the metal-ligand bond is perturbed through spin-delocalization into the conjugated π-system of the mesityl substituent, is strongly bent (M-N-R = 146.5(2)°). Imido complexes with populated *anti*-bonding orbitals of π-symmetry are strongly bent in case of a singlet ground state devoid of strong admixture of excited states. This is the case for the palladium complex **2**(M-N-R = 79.54(9)°)[29],where the intramolecular sulfonate chelate further biases the bent structure.[29] For the closed-shell nickel complexes $\mathbf{4}^{Ter\_Dipp}$ and $\mathbf{4}^{Ter\_Mes}$ with significant triplet-nitrene character (*vide supra*), angles of 147.0(2)° and 127.3(3)° were reported.[32a]

11) Acylnitrenes: While organic azides are commonly used for the synthesis of terminal imido complexes, (di)-oxoazolones have become popular nitrene sources for catalytic C–N and N–N bond formation.[35] The key intermediate of these group 8–11 metal catalyzed reactions are believed to be metalated *N*-acyl-nitrenes (Scheme 1). Acyl nitrenes profit from extensive mesomeric stabilization by the carbonyl substituent. For more details beyond Warren's copper complex and one example in iridium catalysis (*vide infra*, Scheme 16, Scheme 24), we refer the interested reader to a recent review.[48]

Review
doi.org/10.1002/ejic.202100410

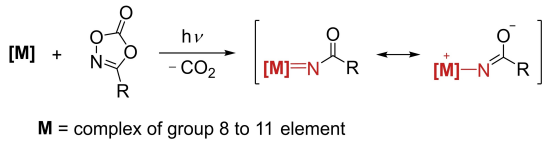

Scheme 1. Formation of imido intermediates by light-induced elimination of CO_2 from dioxoazolones.

3. Group 9 Metals

3.1. Cobalt

Cobalt imido complexes are known since the early 2000s and comparatively well studied.[43,49] Prior to 2013, most complexes featured cobalt in the oxidation state +III and strong-field ancillary ligands, and thus exhibited closed-shell electronic structures (Figure 12, **12**[14], **21**–**25**).[43,49] Compounds **12**[14], **21**–**23** were found to be rather unreactive, which was attributed to their steric protection and the low-spin ground state.[50] Weak electrophilic character was attributed to **12**[49c] and **23**[50–51a] in sight of a sluggish reaction with carbon monoxide. Complexes **21**, where the imido group inserted into the NHC-metal bond likely *via* initial attack at the *p*(z) orbital of the carbene, proved also electrophilic.[49d]

Complexes **23**[50,51] and **14**[44,52] showed thermally accessible open-shell excited states, and **14**^{Mes} exhibited even an intermediate-spin ground state of ($S = 1$). Complex **25** is diamagnetic with an almost linear terminal cobalt imide bond (Co-N-Ad: 172.1°).[53] The combination of a low coordination number and a weak ancillary ligand in **14** results in a compressed ligand field which favors open-shell electron configurations. In 2012, nitrene transfer to phosphine was shown for **14**^{tBu}, and intramolecular H-atom abstraction was found for **14**^{Mes}.[44] Their applications in catalysis and intermolecular C–H functionalization were not reported before 2019. The intramolecular amination of activated benzylic C–H bond in aliphatic azides catalyzed by **14** allowed accessing substituted pyrrolidines (Scheme 2) and illuminated the crucial role of pyridine as solvent. Pyridine coordination prevents the formation of cobalt tetrazene complexes and accordingly enhances the catalyst longevity. Additionally, the presence of pyridine increases the amination rate (k^{obs}), which overall improved the yields from below 10% to 93%.[52]

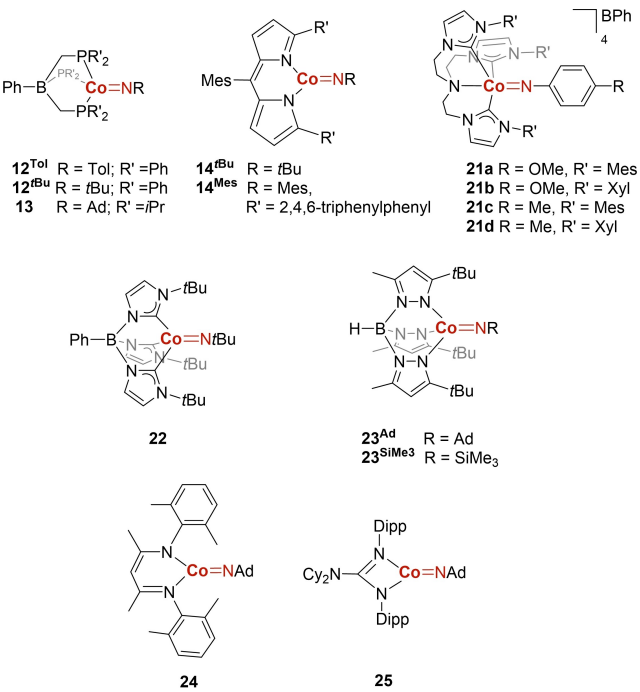

Figure 12. Isolated terminal cobalt imido complexes known until 2013.

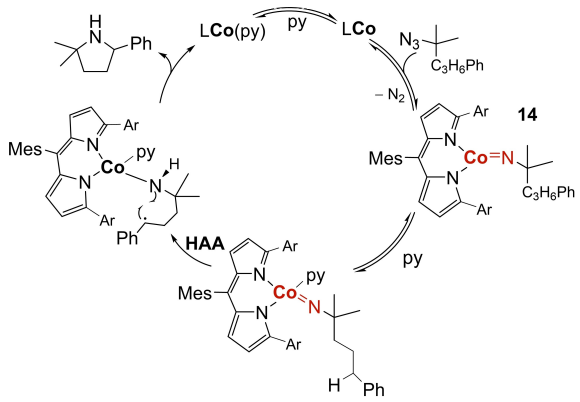

Scheme 2. Intramolecular conversion of alkyl azides to pyrrolidines catalyzed by **14** in pyridine (py). HAA: H-atom abstraction.

The catalytic C–H amination proved to be sensitive to the steric demand of the ancillary ligand. Exchanging the 2,4,6-triphenylphenyl side groups of **14** by a sterically more encumbering trityl substituent (**26**) pushes the imido group into a perpendicular position regarding the plane defined by the dipyrrinato ligand (Figure 13). While the bulky trityl substituents prevent catalyst inhibition in the form of cobalt tetrazido complex, the bent geometry enhances the C–H amination efficiency. The unusual perpendicular arrangement between the imido- and dipyrrinato ligands leads to increased oxidation potential and higher reaction rates.[54]

Arguably taking inspiration from previous work with iron,[55] Mindiola and colleagues targeted to synthesize the cobalt(IV) imido complex **27** (Scheme 3).[56] Complex **27** contains an

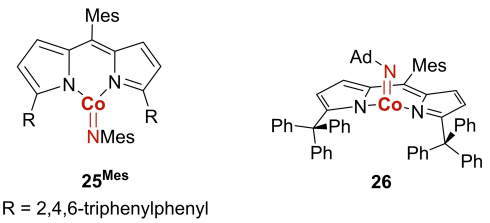

Figure 13. Left: **25**^{Mes}, "in-plane" imido ligand. Right: **26**, "out-of-plane" imido ligand.

Review
doi.org/10.1002/ejic.202100410

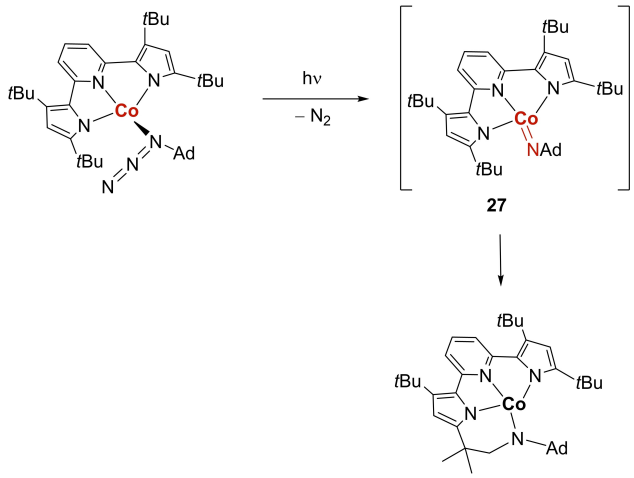

Scheme 3. Proposed cobalt(IV) imido intermediate **27**.

unpaired electron in the imido's π*-*anti*-bonding orbital, thus rendering it more reactive. Indeed, **27** proved to be unstable at room temperature, and instead an intramolecular C–H insertion product was isolated (Scheme 3).

The presence of a transient four-coordinated cobalt imido intermediate (**28**) was further proposed by Caulton and colleagues[57] who isolated the product of intramolecular insertion of the imido group into the cobalt–phosphorus bond (Scheme 4).

The first isolable square planar cobalt(II) imido complex was reported by Chirik and co-workers in 2021.[58] The solid-state structure revealed a long Co–N bond (1.716(2) Å) and a near-to-linear Co–N–C linkage (176.46 (19)°) (Scheme 5). An intermediate spin state ($S=1$) was found and further corroborated by CASSCF(12,8) calculations, which suggest ferromagnetic coupling of a cobalt(II) ion with a radical predominately residing on the imidyl nitrogen. Complex **29** is surprisingly stable; yet, heating to 80 °C for 30 minutes leads to the selective *N*-migratory insertion into the Co–P bond.

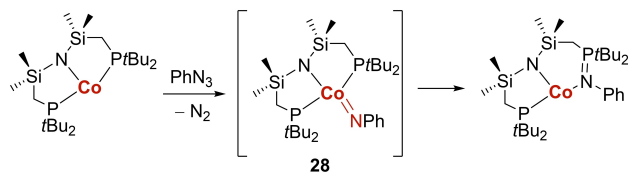

Scheme 4. Proposed cobalt(III) imido complexes **28**.

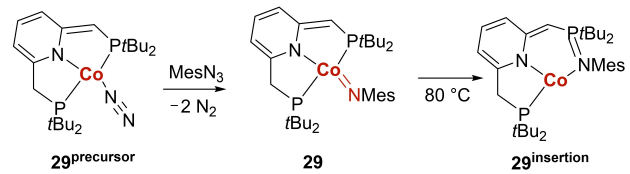

Scheme 5. Synthesis and reactivity of square-planar cobalt imido complex **29**.

Werncke and co-workers isolated the anionic cobalt(III) imido complex **15** with two bistrimethylsilylamido ancillary ligands (Figure 14, left).[59] With 1.7067(12) Å, complex **15** exhibits a rather long Co–N bond. For comparison, in **14**^{tBu}, which represents the shortest bond, 1.609(3) Å was found.[44] The authors attributed the longer bond length to the anionic charge of the complex and the intermediate-spin triplet ground state ($S=1$). Further note the Co–N–C angle of 160.78(12)°, which deviates considerably from linearity.

Analogous to complexes **14**, also **15** abstracts H-atoms from C–H bonds (BDE <92 kcal mol^{-1}).[59] In a subsequent combined experimental and computational study, related aryl congeners **30** were described (Figure 14, right).[60] The electronic structure of these complexes was interpreted as imidyl complexes based on a low (0.6) Co–N and high (1.3) N–C bond order and high spin density at the imido nitrogen atom (0.8 a.u.). These complexes also feature near-to-linear Co–N–C linkages (Co-N_{Mes}-C: 168.9(1)°; Co-N_{Dipp}-C: 178.8(2)°), remarkably long Co–N bonds (Co–N^{Mes}: 1.752(2) Å, Co–N^{Dipp}: 1.751(2) Å), and abstract hydrogen atoms from cyclohexadiene ($BDE=76$ kcal mol$^{<-M>1}$).[60]

The d^7 configured cobalt complexes are rather unusual. The first low-spin trisphosphine cobalt(II) imido complex **5** was reported in 2017 by Deng and colleagues.[61] (For a detailed discussion on the electronic structure see Figure 6 above). Complex **5** shows ambiphilic reactivity and *N*-group transfer with trimethylphosphine as well as with carbon monoxide. Additionally, interesting imido/oxo and imido/sulfido exchange reactions were observed in the presence of benzaldehyde and carbon disulfide (Scheme 6).

Following the nickel complex **8**, linear, di-coordinated cobalt(II) imido complexes **11** were isolated (Figure 15).

The d^7 configured complexes are stabilized by the NHC ancillary ligand IPr (**11**).[42] For the derivatives **11'** and **11''**, unsaturated NHCs were chosen. Solution magnetic susceptibility measurements assigned an $S=3/2$ ground state to complexes **11**, which was further corroborated by DFT

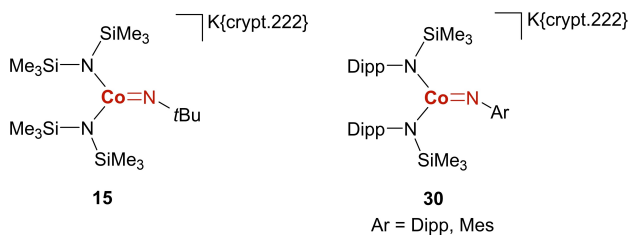

Figure 14. Anionic cobalt(III) imido complexes **15** and **30**.

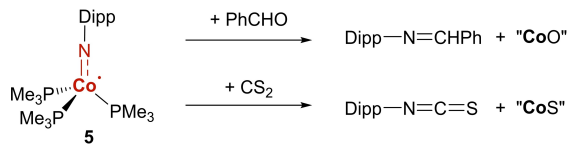

Scheme 6. Exchange reactions of imido ligand in **5** with benzaldehyde and carbon disulfide.

Review
doi.org/10.1002/ejic.202100410

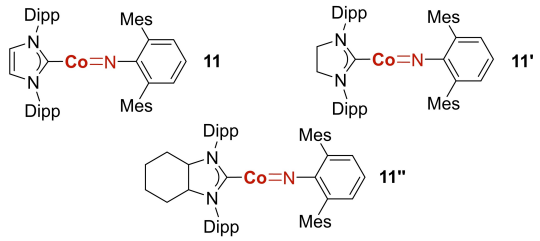

Figure 15. Two-coordinated d^7 cobalt imido complexes.

calculations.[42] The high-spin configuration is in agreement with fairly long Co–N bonds (average for 11: 1.68 Å).[62] The imido ligand in **11** gives isocyanate with carbon monoxide, reacts with terminal alkynes and silanes *via* 1,2-addition, and shows C–H insertion with ethylene (Scheme 7).[42]

Compounds **11** excel with their magnetic properties and represent a new class of single-molecular magnets (SMMs) that exhibit metal-ligand multiple bonds (Figure 16). In fact, **11'** set a new record for transition metal-based SMMs in terms of the effective relaxation barrier (413 cm^{-1}).[62]

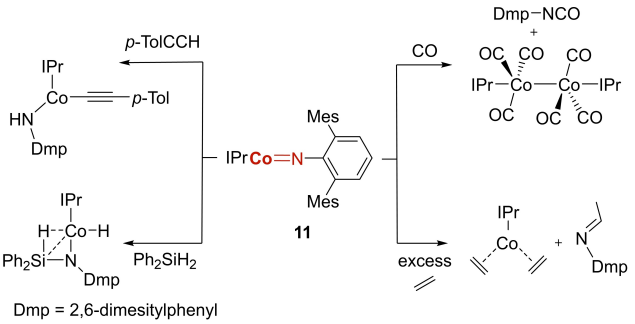

Scheme 7. Bond activation with **11**.

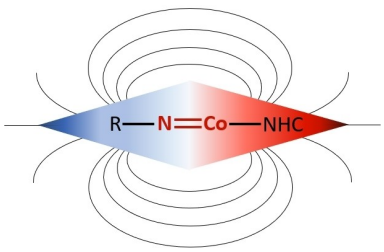

Figure 16. Complexes are single-molecule magnets (SMMs).

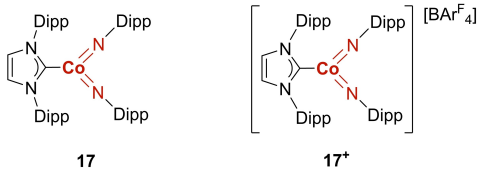

Figure 17. Cobalt(IV)- and cobalt(V) bisimido complexes.

The steric bulk of the imido ligand's substituent is thereby crucial to avoid the formation of bisimido complexes. Accordingly, Deng's group pushed the field through isolating formal cobalt(IV) (**17**) and cobalt(V) (**17**$^+$) bisimido complexes, both of which showed low-spin ground states (Figure 17).[46] The pentavalent complex, stabilized by two π-donating imido ligands, thereby proved remarkably unreactive.

In fact, intramolecular C–H activation was observed only for the d^5 configured ($S = 1/2$) cobalt(IV) complex and DFT calculations suggested significant covalent character only for the formal cobalt(IV)-, but not the cationic cobalt(V) complex.

Although the focus is arguably shifting to imido complexes in two-fold symmetry, complexes in trigonal symmetry continue to attract attention. Thomas and colleagues reported the bimetallic zirconium(IV)/cobalt(II) diimido complex **31**, which was obtained upon treating the reduced heterobimetallic complex with two equivalents of mesityl azide (Scheme 8).[63]

A remarkable achievement was the isolation of a pair of formal cobalt(III/IV) terminal imido complexes (**16**) by Meyer and co-workers.[45] Switching from an ethylene- (*cf.* 21) to a methylene bridged, amino-anchored trisNHC ligand rendered the formal cobalt(IV) complex sufficiently stable to be isolable in the cold at −25 °C (Figure 18).

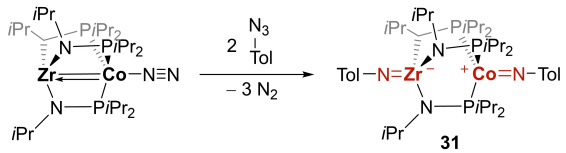

Scheme 8. Mixed zirconium cobalt diimido complex **31**.

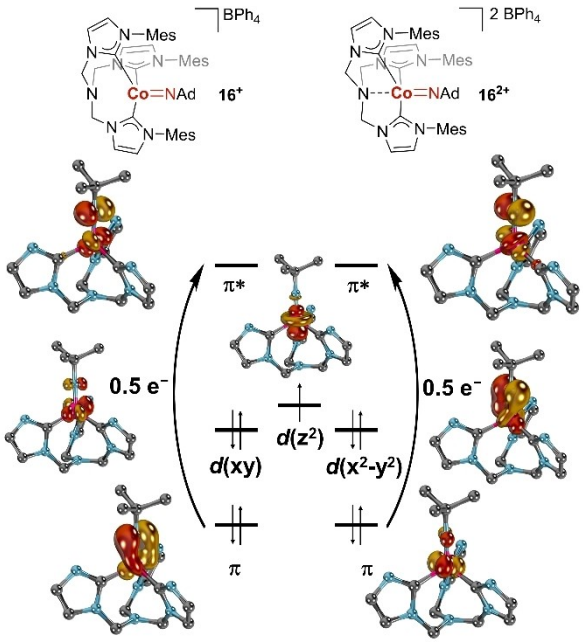

Figure 18. Complexes **16**$^+$ and **16**$^{2+}$ (top) and the electronic structure of **16**$^{2+}$ (bottom). Adamantyl- and mesityl substituents as well as hydrogen atoms are omitted for clarity.

Both these complexes share a low-spin ground-state (16^{+}: $S=0$; 16^{2+}: $S=1/2$). In **16**, the amine of the supporting ligand assumes an unusual trigonal-planar structure due to negative hyperconjugation with the methylene groups and repulsive electrostatic interaction with the cobalt's $d(z^2)$ orbital, which mixes with the 4*s* and 4*p*(z) orbitals. Upon oxidation of $\mathbf{16}^{+}$ to $\mathbf{16}^{2+}$, one electron is removed from the $d(z^2)$ orbital, which attenuates its *anti*-bonding interaction with the imido ligand, and thus also allows the ligand's nitrogen atom to approach the metal ion closer. Complex $\mathbf{16}^{2+}$ is a "textbook" example for a highly covalent imido–metal bond, which is transitioning from a "classic" cobalt(IV) imido- to a triplet-nitrene ligand electronic structure. According to CASSCF calculations, the π-bonds, which are composed of the imido's *p*(x) and *p*(y) and the metal's *d*(xz) and *d*(yz) orbitals, are evenly distributed between the metal and ligand (metal:ligand = 1:1). Thereby, the *anti*-bonding combination is essentially as much populated as the bonding interaction (0.5 a.u. each). This translates, as likewise indicated by a weight of the "imido" lead configuration of only 46%, into substantial nitrene- (30%) and imidyl (18%) character.

The κ-*N* ligated nitrilimido cobalt complex **32** was reported, which formed through salt metathesis of a cobalt(II) precursor ($\mathbf{32}^{\text{precursor}}$) with the lithium salt of trimethylsilyl diazomethane (Scheme 9).[64] In line with a long Co–N bond of 1.914(2) Å, comparable to that of complex $\mathbf{30}^{\text{Mes}}$,[60] the DFT analysis suggests weak multiple bond character with a bond order of only 1.2. The desilylation of **32** triggered the rearrangement to the isocyanoamido complex $\mathbf{32}^{\text{re}}$ in contrast to the iron congener, which formed the terminal nitrido complex.[65] Related κ-*N* bonded diazene ligands have also been reported for iridium.[66] Note in this context that N–N bond activation of hydrazido complexes has been studied in the context of "masked metallanitrene" ligands of early transition metals;[67] however, to the best of our knowledge, this concept has not found application for late transition metals yet.

Hitherto, only one square-planar, tetracoordinated cobalt imido complex (**29**) is known and complexes in octahedral geometry proved to be too reactive to be stable at room temperature.[1,3h] However, their transient existence has been invoked in catalysis and photochemistry.[68] In 2011, Zhang, de Bruin and colleagues reported the first spectroscopic indication for the presence of a porphyrin cobalt(III) imido complex in square-pyramidal coordination geometry (**33**) by *in-situ* EPR spectroscopy (Scheme 10). According to calculations, the unpaired electron resides almost exclusively on the nitrogen atom of the imido moiety.[68c]

A more detailed characterization of **33**, the radical key intermediate for the catalytic C–H bond amination of benzylic C–H bonds with organic azides, followed in 2015.[69] In addition to the mono-radical complex with structural similarity to **33**, the authors also invoked the formation of radical complexes starting from iminoiodanes (Scheme 11).

Interestingly, organic azides led to the mono-radical **34**, but the iodine(III) reagents afforded the octahedral cobalt(III) bis-nitrene complexes **35** instead. The non-innocence of the porphyrin ligand is essential for the formation of **35** which incorporates, as **34**, a cobalt(III) core and additionally a one-electron oxidized ligand. The nature of the ligand L of compound **34** is unclear, but was proposed to be an amino donor ligand. The mono- and bis-imido complexes were studied by DFT methods, EPR and X-ray Absorption Near Edge

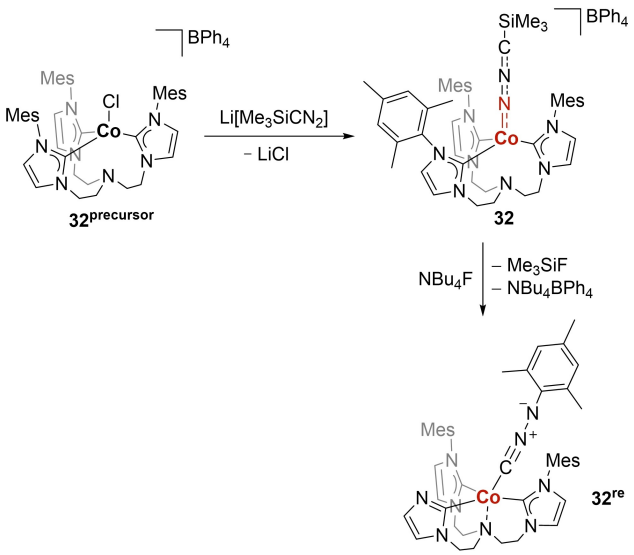

Scheme 9. Synthesis of nitrilimido complex **32** and rearrangement to isocyanoamido complex $\mathbf{32}^{\text{re}}$.

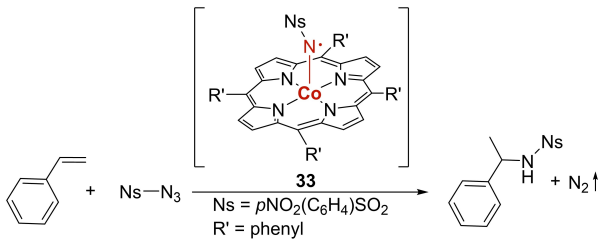

Scheme 10. Proposed square-pyramidal cobalt imido intermediate.

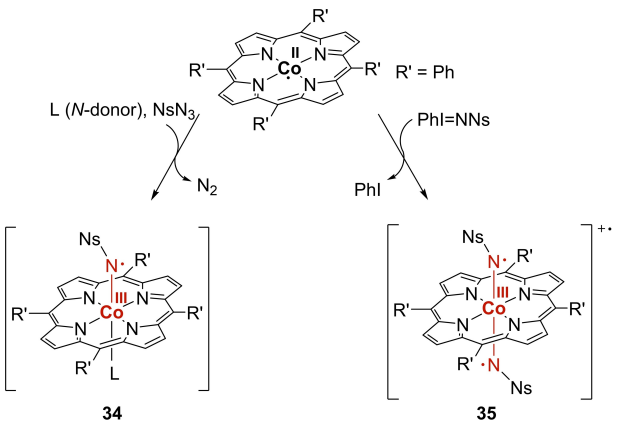

Scheme 11. Cobalt(III) mono- and bis-imido complexes obtained from organic azide (**34**) or *N*-nosyl iminoiodane (**35**), respectively.

Spectroscopy (XANES).[69–70] The DFT calculations predict that the spin density is predominantly localized on the imido nitrogen atoms. The EPR signal of the bis-imido complex **35** is hence more complicated and shows a multiline spectrum with hyperfine interactions with two imido- and four porphyrin *N*-atoms and resembles a (net) doublet spin state. Note, DFT suggested nearly equal energies for the doublet ($S = 1/2$) and quartet ($S = 3/2$) spin states. The intensities of the mono-imido signals in **34** were found to be high and further increased upon heating. Under the same conditions (45 °C, 12 h) the bis-imido complex **35** seemed to decompose in the absence of substrates such as styrene. XANES data suggest a six-coordinated complex and similar average bond distances between cobalt and the ligands, in both cases. This observation rationalizes why additives were found to have little influence on the catalytic properties of **33**.[68b,69–71]

Another bis-imido complex (**36**) was reported by de Bruin and colleagues (Figure 19) along with a reactivity study, which established these complexes as efficient catalysts for chemo- and diastereoselective aziridination of styrene derivatives, cyclohexene and 1-hexene. The catalytic reactions were performed under aerobic conditions.[68e]

For complex **38**,[72] Piers and co-workers observed a similar EPR signal as had been found for **33**.[68c] Accordingly, it was suggested that complex **38** is the key intermediate for the formation of the octahedral cobalt(III) amido complex **39** from **37** (Scheme 12). While the Co(III) imido complex **38** could not be isolated, its presence was further substantiated by DFT calculations.[72]

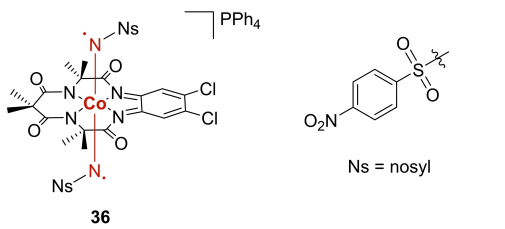

Figure 19. Bis-imido cobalt(III) intermediate **36**.

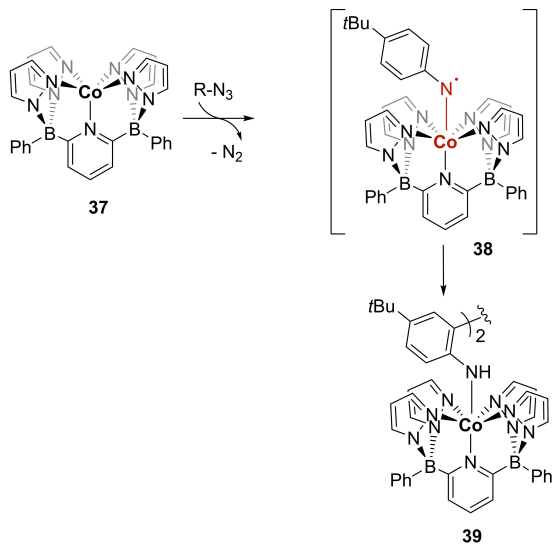

Scheme 12. Proposed octahedral cobalt imido intermediate **38**.

3.2 Rhodium

In contrast to cobalt, only a few terminal imido complexes of rhodium are known. Based on previous work,[73] the catalytic amidation of 2-phenylpyridine in the presence of tosyl azide *via* the cationic rhodium complex **40**^{precursor} was reported (Scheme 13).[74] The proposed key intermediate [(Cp*)Rh=NTs] (40) parallels a compound discussed in an early study by Hursthouse and colleagues.[73]

Hitherto, three isolable terminal rhodium imido complexes have been reported (Scheme 14).[75] All incorporate an anionic trisphosphinoborane ancillary ligand, which has also been utilized to isolate the isoelectronic, diamagnetic d^6 configured cobalt complexes **12**. Indeed, complexes **18** and **12** share comparable electronic structures. In both cases, M-N-C (M = Rh or Co) is arranged linear and DFT calculations indicate two π-bonds and additional symmetry allowed mixing of the vacant metal's *p*(z) with the occupied *d*(z^2) orbital (*vide supra*, Figure 3). Overall, the authors suggested to consider the M–N interaction as a triple bond.[75]

Transient (di)-rhodium imido complexes are alleged key intermediates in catalytic C–H bond amination in organic synthesis[68a,76] and the isolation of these complexes had been a

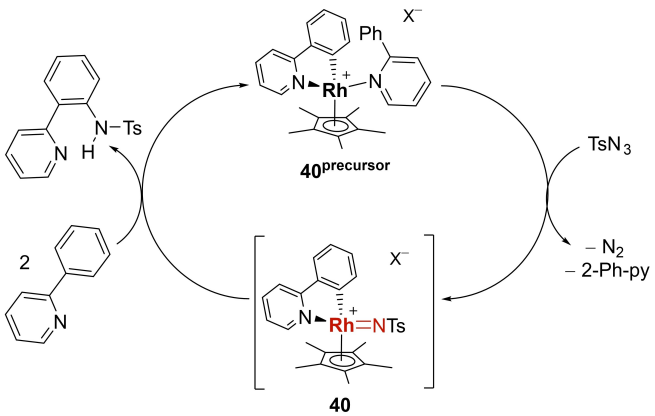

Scheme 13. Catalytic C–H amination *via* transient rhodium imido complex **40**.

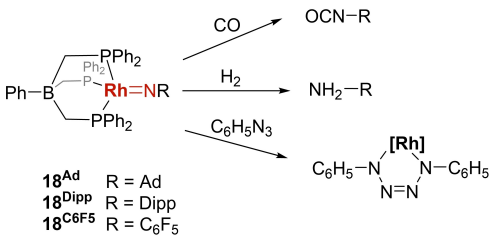

Scheme 14. Terminal rhodium imido complexes **18** react with carbon monoxide, dihydrogen and potentially a further equivalent of organic azide.

long-standing challenge. Until 2018, only a desorption ionization mass spectrometry experiment[77] and computational studies gave indication for their intermediacy.[78] Powers and colleagues presented spectroscopic proof[79] for the formation of a rhodium imido complex in 2018 and managed to crystallize the adamantyl imido compound **19** one year later (Figure 20).[80]

Compound **19** proved to be inactive for C–H amination. However, the authors managed to "follow" the *in-crystallo* synthesis of carbazole from biphenyl azide through intramolecular C–H bond amination *via* the dirhodium imido complex **41**. For that purpose, a single crystal of **41**^{azido} was photolyzed at low temperature (100 K) and refined X-ray crystal structures were periodically obtained using synchrotron radiation (Scheme 15).[81]

3.3. Iridium

Succeeding the early reports by Stone, Basolo and coworkers,[82] Bergman and colleagues presented evidence for a diamagnetic d^6 iridium(III) complex in 1989. The solid-state structures of compounds **42** revealed a linear coordination of a pentamethylcyclopentadienyl (Cp*) and the imido moieties. These complexes are characterized by short Ir–N bonds (average: 1.74 Å) and a near-to-linear Ir-N-C linkage (average: 174.2°), which is indicative of strong multiple bonding, inferred by the authors as a triple bond (Figure 21).[83]

N-Group transfer to carbon monoxide, iodomethane or pivalonitrile, [2 + 2]-cycloaddition with carbon dioxide or alkynes, and the addition of 1,2-bis(diphenylphosphanyl)ethane (dppe) were later reported.[83] The exchange reaction with aryl azides afforded the diisopropylphenyl (**42**^{Dipp}) and 2,6-xylyl (**42**^{xyl}) imido complexes. The addition of excess *tert*-butyl azide, as well as mesityl azide[73], led to the corresponding metalla tetrazenes.[84]

(Cp*)Ir complexes entered C–H amidation catalysis of arenes and alkenes in 2013,[85] and a variety of aromatic and aliphatic azide precursors were applied for the same (Scheme 16). All these complexes share the electron withdrawing acyl motif (*vide supra*), which balances the nucleophilicity of the alleged terminal imido intermediate **43**.

Chang and colleagues further succeeded in the catalytic amidation of sp^3 configured C–H bonds using, *e.g.*, *p*-toluenesulfonyl azide as nitrogen source and $[(Cp^*)IrCl_2]_2$ as catalyst (Scheme 17). Note that the nucleophilic imido group is also in this case stabilized by an electron-withdrawing, namely sulfonyl, group. This catalytic protocol allowed for convenient late-stage C–H amidation with high functional group tolerance.[86]

The catalytic intramolecular C–H amination of aryl azides by iridium(IV) complexes with tetradentate salen (*N*,*N*′-bis(salicylidene)-ethylenediamine) ligands **44**^{precursor} was reported in 2019.[87] The authors suggested the presence of an iridium imido intermediate based on high-resolution ESI-MS analysis (Scheme 18).

Intriguingly, **44** would exhibit a highly unusual octahedral geometry. Scheme 24 displays the proposed reaction mechanism. Compound **44** mediates nitrene insertion into the C–H bond followed by iridium catalyzed dehydrogenation and the release of quinazolinones.

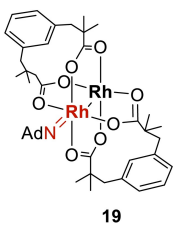

Figure 20. Structure of dirhodium adamantyl imido complex **19**.

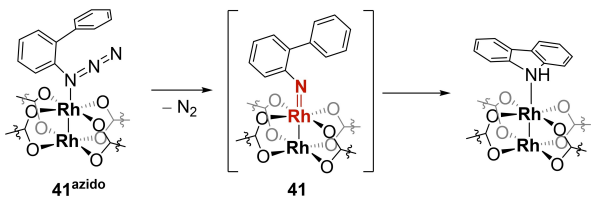

Scheme 15. *In-crystallo* conversion of **41** to amine complex.

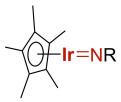

42^{tBu} R = *t*Bu
42^{SiMe3} R = $SiMe_3$
42^{Dipp} R = Dipp
42^{xyl} R = Xyl

Figure 21. Iridium(III) imido complexes known until 2013.

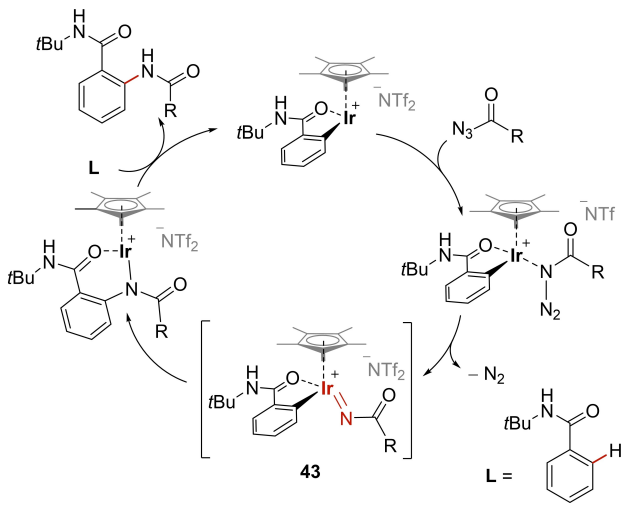

Scheme 16. Iridium catalyzed C–H amidation *via* the transient iridium(IV) terminal imido complex **43** with a Cp* ancillary ligand.

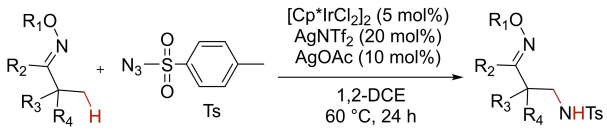

Scheme 17. C–H amidation *via* transient iridium imido complex.

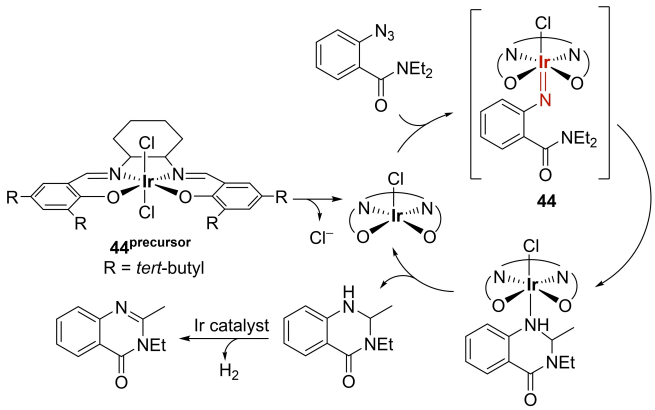

Scheme 18. Iridium catalyzed conversion of aryl azides to quinazolinones.

Apart from Bergman's linear iridium(III) imido complexes **42**, another ligand platform has found application, namely the PNP pincer shown in Scheme 19.[70,88]

Using this supporting ligand, a redox series containing iridium in the oxidation states +III to +V was established. The imido ligand in **20** was interpreted as a triplet-nitrene, and DFT calculations further corroborated that **20** feature two unpaired electrons in the two nearly degenerate π*-orbitals.[88] The one-electron oxidation gives monocationic $\mathbf{20}^{+}$, best described as imidyl complex. Further oxidation led to the dicationic complex $\mathbf{20}^{2+}$.[89] Complexes $\mathbf{20}^{+}$ and **20** were characterized by single-crystal diffractometry and confirmed the unusual near-to-square-planar coordination geometry. The shorter Ir–N bond and a rather linear Ir-N-C group in $\mathbf{20}^{+}$ [1.805(2) Å/171.3(3)°] are in agreement with the presumed electronic structure and a stronger π-bonding in $\mathbf{20}^{+}$ compared to **20** [1.868(2) Å/157.2(2)°]. Despite the radical nature of $\mathbf{20}^{+}$, it was found to be remarkably inert, while *N* -group transfer to carbon dioxide and trimethylphosphine were observed for **20**.

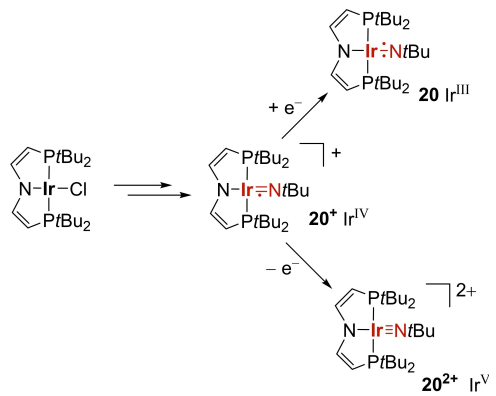

Scheme 19. Iridium(III/IV/V) imido redox series.

4. Group 10 Metals

4.1. Nickel

In analogy to group 9, where cobalt received the most attention, the majority of reports for group 10 relate to the 3*d* element nickel. This is well-illustrated by the work of Hillhouse and colleagues (**3**; Scheme 20, top left)[90a–d] as well as the work by Warren (**45**; Scheme 20, top right).[90e] In particular, the nickel (II) imido complexes **3** showed rich transfer reactivity (Scheme 20, bottom).[32b,c, 47, 90]

In 2013, Harrold and Hillhouse contributed the bent nickel (II) imido complexes $\mathbf{4}^{\text{Ter\_Dipp}}$ and $\mathbf{4}^{\text{Ter\_Mes}}$ stabilized by a bulky chelating di(NHC) ligand with *tert*-butyl "wingtips" and likewise bulky trityl imido substituents (Scheme 21).[32a] The solid-state structures of $\mathbf{4}^{\text{Ter\_Mes}}$ and $\mathbf{4}^{\text{Ter\_Dipp}}$ revealed, compared to $\mathbf{6}^{\text{Ad}}$ and $\mathbf{6}^{\text{Mes}}$ (*vide infra*), slightly elongated Ni–N bonds ($\mathbf{4}^{\text{Ter\_Mes}}$: 1.732(3) Å; $\mathbf{4}^{\text{Ter\_Dipp}}$: 1.718(2) Å) and a remarkably bent Ni-N-C arrangement ($\mathbf{4}^{\text{Ter\_Mes}}$: 127.3(3)°; $\mathbf{4}^{\text{Ter\_Dipp}}$: 147.0(2)°; *cf.* Figure 10). The attempted synthesis of the nickel(III) complex through one electron oxidation of $\mathbf{4}^{\text{Ter\_Mes}}$ led to dehydrogenative C–C coupling at the *para*-position of the diisopropylphenyl substituents and the formation of the dimer $\mathbf{4}^{\text{dimer}}$ (Scheme 21).[32a] Notably, equivalent reactivity had been reported by Sharp on bridging rhodium imido complexes.[91]

Betley and co-workers reported rare examples of nickel(III) imido complexes featuring a bidentate ancillary ligand and an adamantyl-($\mathbf{6}^{\text{Ad}}$) or mesityl-imido ($\mathbf{6}^{\text{Mes}}$) moieties(Figure 22).[36]

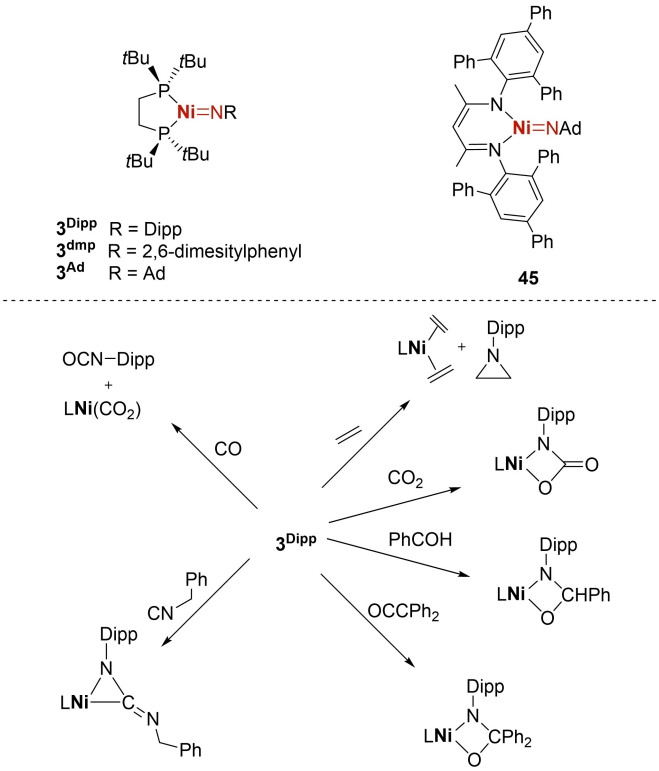

Scheme 20. Top: Nickel imido complexes **3** and **47**, which were reported prior to 2013. Bottom: Small molecule reactivity of $\mathbf{3}^{\text{Dipp}}$.

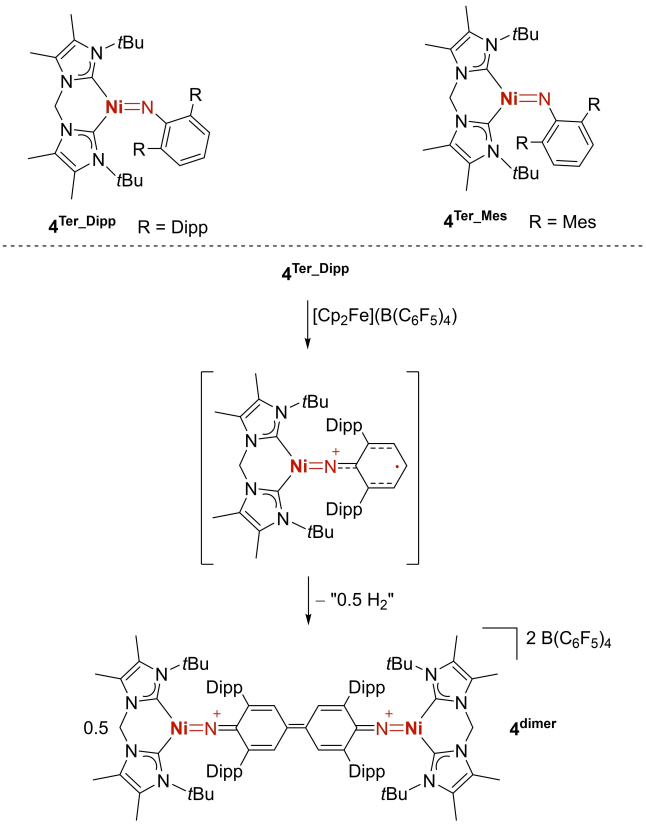

Scheme 21. Dimerization of 4^{Ter_Dipp} upon oxidation.

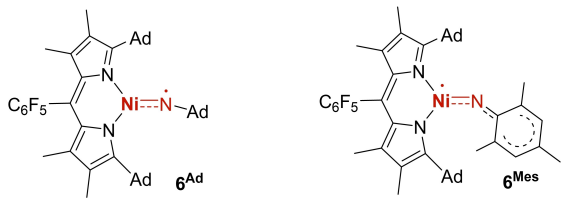

Figure 22. Nickel complexes 6^{Ad} and 6^{Mes} share mixed imido and imidyl characters.

The dipyrrinato ligand contains two bulky adamantyl side chains and additionally a pentafluorophenyl substituent. The Ni–N bond lengths (6^{Mes}: 1.696(2) Å and 6^{Ad}: 1.642(7) Å) are in the same range as found in Hillhouse' NHC supported complexes,[32b,90a–c] with a Ni-N-C angle in 6^{Mes} of 146.5(2)° and 164.8(17)° in 6^{Ad} (*cf.* Figure 11). Accordingly, a shorter metal-nitrogen bond along with a more linear Ni-C-N linkage of 164.8(17)°, indicating stronger multiple bonding, is displayed by the mesityl imido complex 6^{Ad}. The mesityl complex can be understood as "in between a nickel(III) imido and a nickel(II) iminyl complex", while the adamantyl complex was designated to be a nickel(II) imidyl complex (*vide supra*, Figure 6).

The aliphatic imidyl complex 6^{Ad} proved more active in C–H amination than the aryl congener 6^{Mes}. For instance, 6^{Ad} activated the benzylic position in toluene to give the corresponding imine as product, along with the nickel amido complex (Scheme 22). The authors attributed the lower reactivity of 6^{Mes} to the larger spin concentration on nickel.

Catalysts **6** allow for C–H amination and share similar reactivity with the previously studied cobalt imido complexes **14** (*cf.* Scheme 2). Subsequent work established the catalytic conversion of aliphatic azides bearing a benzylic position *via* C–H amination, intramolecular ring closure and elimination of pyrrolidine derivatives.[92]

Betley and co-workers introduced the nickel imidyl catalyst **46** with a monoanionic bisoxazoline (BOX) ligand featuring bulky trityl-substituents (Figure 23).[93] The solid-state structure of 46^{Ad} showed a Ni–N bond length of 1.680(8) Å, similar to those of 6^{Ad} and 6^{Mes}. The asymmetric unit of 46^{Ad} contained two molecules with strongly differing Ni-N-C angles, 139.5(7)° and 152.8(8)°, which the authors attributed to crystal packing effects. The observed structural data are in line with the calculated radical character with the spin density residing predominately on the imido nitrogen atom (SOMO: Ni 33%, N^{Ad} 52%). In analogy to complexes **6** and **18**, 46^{Ad} catalyzes the enantioselective intramolecular conversion of alkyl azides to pyrrolidines. However, contrarily to the former complexes, it does so enantioselectively (*ee* up to 79%) due to the chiral BOX ligand.

4.2. Palladium

Palladium imido species are the suggested key intermediates in catalytic C–H amination transformations.[94] The first isolated palladium(II) imido complex was reported in 2018[29] following a detailed computational investigation on how to tame palladium terminal oxo and imido complex.[95] The elucidated trends of this study suggested an ancillary strong-field ligand in combination with an electron-withdrawing imido moiety for attenuation of the imide's nucleophilicity. Accordingly, a cyclic(alkyl)(amino) carbene (CAAC) ancillary ligand, being a strong σ-donor and π-acceptor, and an electron-withdrawing sulfonyl substituent, as had been previously applied for C–H amidation catalysis,[96] was chosen. In the solid state, a weak coordinative interaction between the palladium metal and one oxygen atom of the

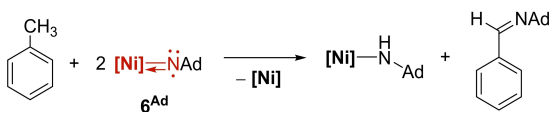

Scheme 22. C–H functionalization by 6^{Ad}.

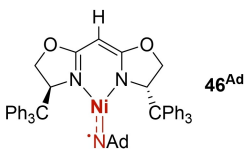

Figure 23. Enantiopure bisoxazoline ligated nickel imidyl catalyst 46^{Ad}.

sulfonyl group (Pd–O bond: 2.1027(17) Å, calculated bond order: 0.5) was found, which further stabilizes **2** (Figure 24).[29]

The closed-shell d^8 complex **2** features a populated π-*anti*-bonding HOMO and an unusual zwitterionic electronic structure (*cf.* Figure 4). The imido complex is very nucleophilic as evidenced by the swift coordination of potassium cations to the imide,[97] yet was shown to give the iminophosphorane as well with trimethylphosphine. The activation of H–H, O–H, N–H and C–H bonds *via* 1,2 addition as well as catalytic hydrogenation of azides with dihydrogen was demonstrated.[29]

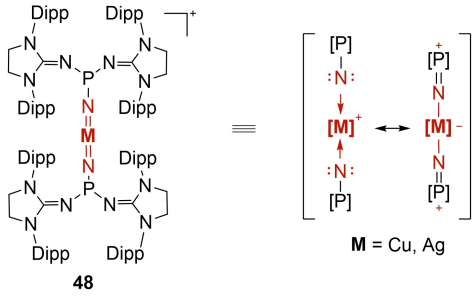

Figure 26. Copper and silver bisimido complexes 48.

4.3. Platinum

Formal multiple bonds with platinum are exceedingly rare.[98] In 2019, the platinum(II) complex **47** with two ketimide ligands was isolated.[99] It represents not only the first linear two-coordinated platinum(II) complex, but also shows remarkable short Pt–N bonds of 1.815(4) Å and 1.818(4) Å (Figure 25). The stability of the linear coordination geometry was ascribed to the strong-field ketimide ligands, which allow for a highly covalent Pt–N interaction due to strong π-donor and π-acceptor properties. The short Pt–N bond and the significant deshielding in the NMR experiment observed for platinum (^{195}Pt chemical shift: $\delta^{Pt} = -629$ ppm; normal range for Pt^{II} complexes with nitrogen-based ligands −2700 to −1700 ppm) along with a large coupling constant ($J^{Pt-N} = 537$ Hz) indicate non-negligible multiple bond character. Note, while Hillhouse's linear nickel(II) imido complexes exhibits a triplet ground state, (*cf.* Figure 7),[11] a diamagnetic ground state was found for **46**.[99]

5. Group 11 Metals

Among coinage metals, copper seems better studied in comparison to silver and gold. Copper-imido intermediates have been proposed and studied in catalytic nitrene transfer; yet[100] isolated examples remain exceedingly rare. Bertrand and co-workers reported copper- and silver bisimido complexes **48** (Figure 26),[48] which however profited from excessive stabilization through conjugation with the imido's substituent, rendering the singlet-nitrene ligand even stable in its free form.[101]

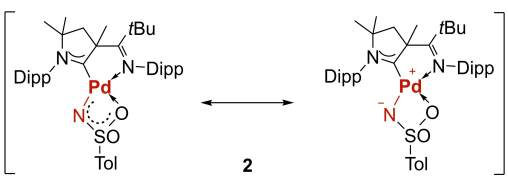

Figure 24. Zwitterionic palladium(II) imido complex **2**.

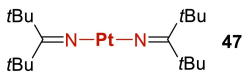

Figure 25. Linear platinum(II) bis(ketimide) complex **47**

Warren and colleagues observed the formation of a dinuclear copper(II) complex (**49**^{dimer}) from copper(I) β-diketiminate in the presence of an arylazide and suggested a mechanism *via* the copper imido intermediate **49** (Scheme 23).[102] The triplet biradical character of **49**^{dimer} was corroborated by EPR and reactivity studies, which revealed *N*-group transfer to trimethylphosphine, *tert*-butyl isocyanide and the benzylic C–H bond of ethylbenzene. Accordingly, the authors suggested **49**^{dimer} as a "masked" terminal copper nitrene.

β-Diketiminato stabilized copper nitrene complexes **50** and **51** were also suggested as key intermediates in catalytic C–H functionalization reactions and catalyst-controlled site-selective C–H amination, respectively (Scheme 24).

50^{precursor} was found to form an isolable dicopper alkylnitrene; however, kinetic studies indicated terminal nitrene **50** as the catalytically competent species.[103] As per this report, bulkier ligands prevent the formation of dinuclear compounds and hence increase the turnover frequency. Acylimido complex **51** does not require directing groups for high regioselectivity in C–H amination catalysis. The sterically demanding β-diketiminato ligand (with *ortho*-diphenylmethyl and *para*-*tert*-butyl substituents) leads to preferential activation of the stronger, yet more exposed, primary or secondary C–H bonds in comparison to the weaker, yet less accessible tertiary C–H bonds.[104]

Betley and co-workers employed a weak-field dipyrrinato ligand, previously used for cobalt and nickel (*vide supra*), as the backbone for complex **7**, yet incorporated significantly enhanced steric bulk (Figure 27).[37]

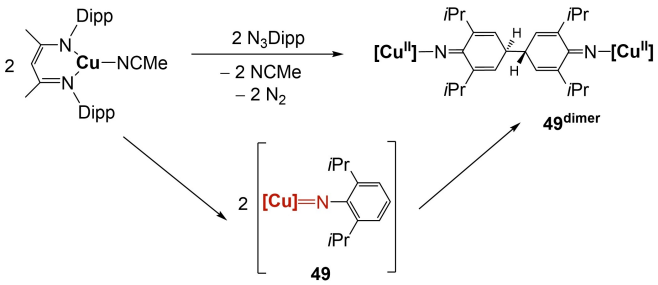

Scheme 23. Formation of dicopper diketimide **49**^{dimer} *via* the intermediate copper imido complex **49**.

Review
doi.org/10.1002/ejic.202100410

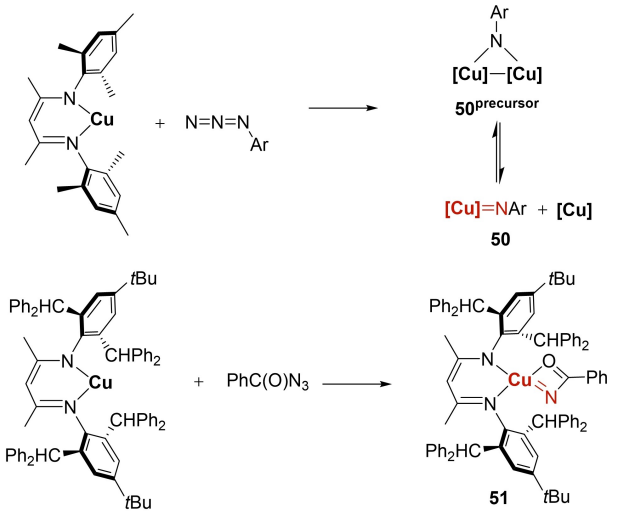

Scheme 24. Cu-nitrenes involved in catalytic C–H functionalization.

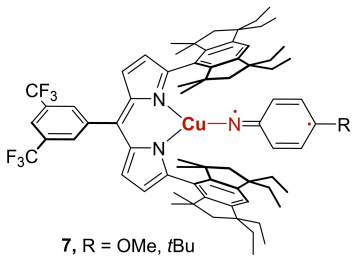

Figure 27. Copper imido complexes **7**.

The use of an aryl imido moiety allowed for the stabilization by delocalizing electron density into the aryl substituent. Computational studies indicated a multiconfigurational ground state with 25% iminyl ligand character and a 58% contribution of a copper(I) triplet-nitrene complex where one radical is located on the imido nitrogen and the second being delocalized within the aryl ligand. Although the short Cu–N bond (1.759(2) Å) in the solid-state indicates at least some multiple bond character, XAS spectroscopy corroborated in agreement with calculations a monovalent copper ion bonded to a subvalent nitrogen atom, *viz.* nitrene (*vide supra*).

The reactivity of complexes **7** can be increased by exchanging the electron-withdrawing 3,5-ditrifluoromethylphenyl- by a mesityl substituent and using electron-poor azides such as hexafluorophenyl azide. Indeed, catalytic nitrene transfer was obtained and the aziridination of styrene, as well as C–H amination of alkanes, was observed.[37] It is interesting to note that this trend is opposed to the common notion that electron withdrawing imido substituents stabilize their complexes (*vide supra*), which thus highlights the electrophilicity of these nitrenes.

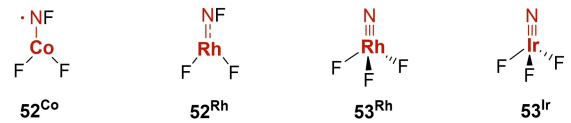

Figure 28. Group 9 metal fluoro nitrenoid **52** and nitride complexes **53**.

6. Gas-Phase and Matrix Studies

Metal oxides and their C–H bond activation reactivity have been intensely studied by mass spectrometry.[105] Among them, CuO^+ has found special attention,[106] and it was shown that the coordination of a further acetonitrile ligand strengthens the Cu–O bond through weakening of the biradical character of the oxygen atom in favor of an oxyl electronic structure.[107] This shift in electronic structures correlates with reduced H-atom abstraction activity. Intriguingly, another study by Schwarz and co-workers established that, contrarily to CuO^+ and AgO^+, AuO^+ reacts with methane exclusively *via* oxygen atom insertion (OAT) and not H-atom abstraction (HAT).[108]

Studies by Schwarz, Beckers and Franger[109] corroborate weak oxygen-metal bonds with calculated bond orders typically below one and significant triplet oxygen character. For the mercury(II) oxyfluoride OHgF, the spin density was calculated to reside exclusively at the oxygen atom. Conversely, dominant oxyl character was found for the group 10 congeners OMF and OMF_2 (M = Ni, Pd, Pt).[110] This very detailed study gauged as well computationally the degree of covalency and orbital inversion in the O–M π-interaction, when moving down the group (3*d*→4*d*→5*d*) and across the period (group 9→group 10→group 11) for isoelectronic complexes. Thereby, a very high degree of inversion was found for group 11, leading to exclusive spin-density at the oxygen ligand. The trends (spin density on oxygen atoms, *d*-electron population) when moving down the group were not entirely consistent and thus suggest a subtle interplay with the enhanced influence of relativistic effects. It seems here interesting to note that a similar reciprocal relationship has been found for group 11 carbene complexes without heteroatom stabilization.[111]

Following previous work on the coinage metals,[112] also fluoroimido- **52** and nitrido complexes **53**[113] of the group 9 were matrix isolated.[114] Fluoroimido complexes of excited cobalt- (rhodium, respectively) atoms with trifluoroammonia NF_3 were trapped in frozen neon or argon (Figure 28). According to high-level calculations, the metal–nitrogen interaction is very covalent and a single bond in case of cobalt, whereas it is a double bond for rhodium. When moving from cobalt to rhodium and especially iridium, the rearrangement of the fluoroimido- to the nitrido complexes becomes increasingly exothermic. Thus, both imido- and nitrido complexes could be studied in case of rhodium, whereas only the latter was obtained for iridium (**53**^{Ir}).

8. Summary and Outlook

The 2010s have brought remarkable progress in the field of imido complexes of late transition metals. Arguably driven by terminal oxo ligands in the bioinorganic chemistry of iron and manganese, and emphasizing open-shell chemistry for catalytic C–H functionalization, the focus was mainly put on the 3*d* metals cobalt, nickel and copper. However, the last few years have seen considerable growth in the chemistry of the heavier 4*d* and 5*d* elements. Whereas *N*-group transfer catalysis by their complexes is emerging, the isolation of the respective reactive intermediates remains largely elusive. Eventually, taking inspiration from *f*-, *s*- and *p*-block- chemistry[115] as well as gas-phase- and matrix experiments, we think that time has come to also consider the group 12 elements and heavy *p*-block metals for certainly exciting synthetic endeavors.

Acknowledgements

Open Access funding enabled and organized by Projekt DEAL.

Conflict of Interest

The authors declare no conflict of interest.

Keywords: Electronic structure · Imido ligands · Late transition metals · Multiple bonds · Nitrene ligands

[1] K. Ray, F. Heims, F. F. Pfaff, *Eur. J. Inorg. Chem.* **2013**, *2013*, 3784–3807.
[2] a) A. Grünwald, D. Munz, *Encycl. Inorg. Bioinorg. Chem.* **2021**, asap.
[3] a) J. Mayer, W. A. Nugent, **1988**, pp. *In Metal-Ligand Multiple Bonds: The Chemistry of Transition Metal Complexes Containing Oxo, Nitrido, Imido, Alkylidene, or Alkylidyne Ligands*, John Wiley & Sons, Inc., **1988**; b) A. R. Eikey, M. M. Abu-Omar, *Coord. Chem. Rev.* **2003**, *243*, 83–124; c) L. H. Gade, P. Mountford, *Coord. Chem. Rev.* **2001**, *216–217*, 65–97; d) C. J. Ballhausen, H. B. Gray, *Inorg. Chem.* **1962**, *1*, 111; e) J. M. Mayer, *Comments Inorg. Chem.* **1988**, *8*, 125–135; f) A. R. Corcos, J. S. Pap, T. Yang, J. F. Berry, *J. Am. Chem. Soc.* **2016**, *138*, 10032–10040; g) J. F. Berry, *Comments Inorg. Chem.* **2009**, *30*, 28–66; h) J. R. Winkler, H. B. Gray, *Struct. Bonding (Berlin)* **2012**, *142*, 17–28.
[4] M. Á. Baeza Cinco, T. W. Hayton, *Eur. J. Inorg. Chem.* **2020**, *2020*, 3613–3626.
[5] a) V. A. Larson, B. Battistella, K. Ray, N. Lehnert, W. Nam, *Nat. Chem. Rev.* **2020**, *4*, 404–419; b) X.-P. Zhang, A. Chandra, Y.-M. Lee, R. Cao, K. Ray, W. Nam, *Chem. Soc. Rev.* **2021**.
[6] K. Meyer, D. Munz, *Nat. Chem. Rev.* **2021**, *5*, 422–439.
[7] a) K. Kawakita, B. F. Parker, Y. Kakiuchi, H. Tsurugi, K. Mashima, J. Arnold, I. A. Tonks, *Coord. Chem. Rev.* **2020**, *407*, 213118; b) R. R. Schrock, *Chem. Rev.* **2009**, *109*, 3211–3226.
[8] For a detailed discussion of the electronic structure of carbene ligands, see: a) T. R. Cundari, M. S. Gordon, *J. Am. Chem. Soc.* **1991**, *113*, 5231–5243; for a concise discussion of the electronic structure of carbene ligands including a a multiconfigurational perspective, see:; b) D. Munz, *Organometallics* **2018**, *37*, 275–289.
[9] a) C. J. Ballhausen, H. B. Gray, *Inorg. Chem.* **1962**, *1*, 111–122; b) A. R. Corcos, J. S. Pap, T. Yang, J. F. Berry, *J. Am. Chem. Soc.* **2016**, *138*, 10032–10040; c) M. P. Mehn, J. C. Peters, *J. Inorg. Biochem.* **2006**, *100*, 634–643.
[10] P. F. Kuijpers, J. I. van der Vlugt, S. Schneider, B. de Bruin, *Chem. Eur. J.* **2017**, *23*, 13819–13829.
[11] C. A. Laskowski, A. J. M. Miller, G. L. Hillhouse, T. R. Cundari, *J. Am. Chem. Soc.* **2011**, *133*, 771–773.
[12] N. D. Harrold, R. Waterman, G. L. Hillhouse, T. R. Cundari, *J. Am. Chem. Soc.* **2009**, *131*, 12872–12873.
[13] a) Y. Wang, M. E. Muratore, A. M. Echavarren, *Chem.* **2015**, *21*, 7332–7339; b) P. J. Perez, A. Caballero, *Chem. Eur. J.* **2017**, *23*, 14389–14393.
[14] C. Wentrup, *Angew. Chem. Int. Ed.* **2018**, *57*, 11508–11521; *Angew. Chem.* **2018**, *130*, 11680–11693; .
[15] G. P. Moss, P. A. S. Smith, D. Tavernier, *Pure Appl. Chem.* **1995**, *67*, 1307–1375.
[16] N. G. Connelly, T. Damhus, R. M. Hartshorn, A. T. Hutton, *Nomenclature of Inorganic Chemistry IUPAC recommendations*, RSC Publishing, **2005**.
[17] The trend for the early transition metals is reversed: W. A. Nugent, R. J. McKinney, R. V. Kasowski, F. A. Van-Catledge, *Inorg. Chim. Acta* **1982**, *65*, L91.
[18] T. R. Cundari, *J. Am. Chem. Soc.* **1992**, *114*, 7879–7888.
[19] For the leading review on inverted, "σ-only" ligand fields, see: a) R. Hoffmann, S. Alvarez, C. Mealli, A. Falceto, T. J. Cahill, T. Zeng, G. Manca, *Chem. Rev.* **2016**, *116*, 8173–8192; for a discussion of inverted ligand fields based on π-interactions, see: b) L. Li, H. Becker, T. Stüker, T. Lindič, T. Schlöder, D. Andrae, S. Riedel, *Inorg. Chem. Front.* **2021**, *8*, 1215–1228; c) J. D. Rolfes, M. van Gastel, F. Neese, *Inorg. Chem.* **2020**, *59*, 1556–1565.
[20] Y. Shimoyama, T. Kojima, *Inorg. Chem.* **2019**, *58*, 9517–9542.
[21] S. K. Singh, J. Eng, M. Atanasov, F. Neese, *Coord. Chem. Rev.* **2017**, *344*, 2–25.
[22] For a detailed discussion, see: Y. Jean, *Molecular Orbitals of Transition Metal Complexes*, Oxford University Press, **2005**.
[23] a) C. R. Landis, T. Cleveland, T. K. Firman, *J. Am. Chem. Soc.* **1995**, *117*, 1859–1860; b) M. Kaupp, *Angew. Chem. Int. Ed.* **2001**, *40*, 3534–3565; *Angew. Chem.* **2001**, *113*, 3642–3677; c) G. Frenking, N. Frohlich, *Chem. Rev.* **2000**, *100*, 717–774.
[24] T. E. Westre, P. Kennepohl, J. G. DeWitt, B. Hedman, K. O. Hodgson, E. I. Solomon, *J. Am. Chem. Soc.* **1997**, *119*, 6297–6314.
[25] a) J.-U. Rohde, T. A. Betley, T. A. Jackson, C. T. Saouma, J. C. Peters, L. Que, *Inorg. Chem.* **2007**, *46*, 5720–5726; b) J. J. Scepaniak, M. D. Fulton, R. P. Bontchev, E. N. Duesler, M. L. Kirk, J. M. Smith, *J. Am. Chem. Soc.* **2008**, *130*, 10515–10517.
[26] G. E. Cutsail, 3rd, B. W. Stein, D. Subedi, J. M. Smith, M. L. Kirk, B. M. Hoffman, *J. Am. Chem. Soc.* **2014**, *136*, 12323–12336.
[27] a) M. Atanasov, D. Ganyushin, D. A. Pantazis, K. Sivalingam, F. Neese, *Inorg. Chem.* **2011**, *50*, 7460–7477; b) B. R. McGarvey, J. Telser, *Inorg. Chem.* **2012**, *51*, 6000–6010; c) M. Keilwerth, L. Grunwald, W. Mao, F. W. Heinemann, J. Sutter, E. Bill, K. Meyer, *J. Am. Chem. Soc.* **2021**, *143*, 1458–1465.
[28] W. A. Herrman, W. Baratta, E. Herdtweck, *Angew. Chem. Int. Ed.* **1996**, *35*, 1951–1953; *Angew. Chem.* **1996**, *108*, 2098–2100.
[29] A. Grünwald, N. Orth, A. Scheurer, F. W. Heinemann, A. Pöthig, D. Munz, *Angew. Chem. Int. Ed.* **2018**, *57*, 16228–16232; *Angew. Chem.* **2018**, *130*, 16463–16467.
[30] C. Limberg, *Angew. Chem. Int. Ed.* **2009**, *48*, 2270–2273; *Angew. Chem.* **2009**, *121*, 2305–2308.
[31] M. T. Whited, *Beilstein J. Org. Chem.* **2012**, *8*, 1554–1563.
[32] a) N. D. Harrold, G. L. Hillhouse, *Chem. Sci.* **2013**, *4*, 4011–4015; b) D. J. Mindiola, G. L. Hillhouse, *J. Am. Chem. Soc.* **2001**, *123*, 4623–4624; c) D. J. Mindiola, R. Waterman, V. M. Iluc, T. R. Cundari, G. L. Hillhouse, *Inorg. Chem.* **2014**, *53*, 13227–13238.
[33] The doubly excited configuration c"(0,2)" was condensed with double weight.
[34] Calculations for $\mathbf{3}^{trunc}$ were run with an (16,12), calculations for $\mathbf{4}^{trunc}$ with an (16,12) activate space. Smaller active spaces lead to consistent results, yet arguably do not adequately include the interaction with the π-system of the aryl imido substituents.
[35] Y. Liu, J. Du, L. Deng, *Inorg. Chem.* **2017**, *56*, 8278–8286.
[36] Y. Dong, J. T. Lukens, R. M. Clarke, S.-L. Zheng, K. M. Lancaster, T. A. Betley, *Chem. Sci.* **2020**, *11*, 1260–1268.
[37] K. M. Carsch, I. M. DiMucci, D. A. Iovan, A. Li, S.-L. Zheng, C. J. Titus, S. J. Lee, K. D. Irwin, D. Nordlund, K. M. Lancaster, T. A. Betley, *Science* **2019**, *365*, 1138–1143.
[38] J. Sun, J. Abbenseth, H. Verplancke, M. Diefenbach, B. de Bruin, D. Hunger, C. Würtele, J. van Slageren, M. C. Holthausen, S. Schneider, *Nat. Chem.* **2020**, *12*, 1054–1059.
[39] For selected work, see: a) A. Doddi, D. Bockfeld, T. Bannenberg, M. Tamm, *Chem. Eur. J.* **2020**, *26*, 14878–14887; b) M. Peters, T. Bannenberg, D. Bockfeld, M. Tamm, *Dalton Trans.* **2019**, *48*, 4228–4238; c) M. Peters, A. Doddi, T. Bannenburg, M. Freytag, P. G. Jones, M. Tamm, *Inorg. Chem.* **2017**, *56*, 10785–10793; d) A. Doddi, D. Bockfeld,

T. Bannenburg, P. G. Jones, M. Tamm, *Angew. Chem. Int. Ed.* **2014**, *53*, 13568–13572; *Angew. Chem.* **2014**, *126*, 13786–13790.
[40] a) A. Doddi, M. Peters, M. Tamm, *Chem. Rev.* **2019**, *119*, 6994–7112; b) X. Wu, M. Tamm, *Coord. Chem. Rev.* **2014**, *260*, 116–138.
[41] M. Toshiyuki, S. Takashi, M. Nishina, D. Yosuke, H. Toshikazu, *J. Inorg. Biochem.* **2020**, *203*, 110880.
[42] J. Du, L. Wang, M. Xie, L. Deng, *Angew. Chem. Int. Ed.* **2015**, *54*, 12640–12644; *Angew. Chem.* **2015**, *127*, 12831–12835.
[43] T. A. Betley, J. C. Peters, *J. Am. Chem. Soc.* **2003**, *125*, 10782–10783.
[44] E. R. King, G. T. Sazama, T. A. Betley, *J. Am. Chem. Soc.* **2012**, *134*, 17858–17861.
[45] W. Mao, D. Fehn, F. W. Heinemann, A. Scheurer, D. Munz, K. Meyer, *Angew. Chem. Int. Ed.* **2021**, *60*, 16480–16486; *Angew. Chem.* **2021**, *127*, 16616–16622.
[46] L. Zhang, Y. Liu, L. Deng, *J. Am. Chem. Soc.* **2014**, *136*, 15525–15528.
[47] V. M. Iluc, A. J. Miller, J. S. Anderson, M. J. Monreal, M. P. Mehn, G. L. Hillhouse, *J. Am. Chem. Soc.* **2011**, *133*, 13055–13063.
[48] F. Dielmann, D. M. Andrada, G. Frenking, G. Bertrand, *J. Am. Chem. Soc.* **2014**, *136*, 3800–3802.
[49] a) Y. Park, S. Chang, *Nat. Catal.* **2019**, *2*, 219–227; b) H. Wang, H. Jung, F. Song, S. Zhu, Z. Bai, D. Chen, G. He, S. Chang, G. Chen, *Nat. Chem.* **2021**; c) D. M. Jenkins, T. A. Betley, J. C. Peters, *J. Am. Chem. Soc.* **2002**, *124*, 11238–11239; d) X. Hu, K. Meyer, *J. Am. Chem. Soc.* **2004**, *126*, 16322–16323; e) X. Dai, P. Kapoor, T. H. Warren, *J. Am. Chem. Soc.* **2004**, *126*, 4798-4799; f) R. E. Cowley, R. P. Bontchev, J. Sorrell, O. Sarracino, Y. Feng, H. Wang, J. M. Smith, *J. Am. Chem. Soc.* **2007**, *129*, 2424–2425.
[50] < >S. Thyagarajan, D. T. Shay, C. D. Incarvito, A. L. Rheingold, K. H. Theopold, *J. Am. Chem. Soc.* **2003**, *125*, 4440–4441.
[51] a) D. T. Shay, G. P. A. Yap, L. N. Zakharov, A. L. Rheingold, K. H. Theopold, *Angew. Chem. Int. Ed.* **2005**, *44*, 1508–1510; *Angew. Chem.* **2005**, *117*, 1532–1534; b) D. T. Shay, G. P. A. Yap, L. N. Zakharov, A. L. Rheingold, K. H. Theopold, *Angew. Chem. Int. Ed.* **2006**, *45*, 7870–7870; *Angew. Chem.* **2006**, *118*, 8034–8034.
[52] Y. Baek, T. A. Betley, *J. Am. Chem. Soc.* **2019**, *141*, 7797–7806.
[53] C. Jones, C. Schulten, R. P. Rose, A. Stasch, S. Aldridge, W. D. Woodul, K. S. Murray, B. Moubaraki, M. Brynda, G. La Macchia, L. Gagliardi, *Angew. Chem. Int. Ed.* **2009**, *48*, 7406–7410; *Angew. Chem.* **2009**, *121*, 7542–7546.
[54] Y. Baek, E. T. Hennessy, T. A. Betley, *J. Am. Chem. Soc.* **2019**, *141*, 16944–16953.
[55] K. Searles, S. Fortier, M. M. Khusniyarov, P. J. Carroll, J. Sutter, K. Meyer, D. J. Mindiola, K. G. Caulton, *Angew. Chem. Int. Ed.* **2014**, *53*, 14139–14143; *Angew. Chem.* **2014**, *126*, 14363–14367.
[56] L. N. Grant, M. E. Carroll, P. J. Carroll, D. J. Mindiola, *Inorg. Chem.* **2016**, *55*, 7997–8002.
[57] M. J. Ingleson, M. Pink, H. Fan, K. G. Caulton, *J. Am. Chem. Soc.* **2008**, *130*, 4262–4276.
[58] Y. Park, S. P. Semproni, H. Zhong, P. J. Chirik, *Angew. Chem. Int. Ed.* **2021**„ *60*, 14376 –14380; *Angew. Chem.* **2021**, *133*, 14497–14501.
[59] A. Reckziegel, C. Pietzonka, F. Kraus, G. Werncke, *Angew. Chem. Int. Ed.* **2020**, *59*, 8527–8531; *Angew. Chem.* **2020**, *132*, 8605–8609.
[60] A. Reckziegel, M. Kour, B. Battistella, S. Mebs, K. Beutert, R. Berger, C. G. Werncke, *Angew. Chem. Int. Ed.* **2021**, *60*, 15376–15380; *Angew. Chem.* **2021**, *133*, 15504–15508.
[61] Y. Liu, J. Du, L. Deng, *Inorg. Chem.* **2017**, 8278–8286.
[62] X.-N. Yao, J.-Z. Du, Y.-Q. Zhang, X.-B. Leng, M.-W. Yang, S.-D. Jiang, Z.-X. Wang, Z.-W. Ouyang, L. Deng, B.-W. Wang, S. Gao, *J. Am. Chem. Soc.* **2017**, *139*, 373–380.
[63] B. Wu, R. Hernández Sánchez, M. W. Bezpalko, B. M. Foxman, C. M. Thomas, *Inorg. Chem.* **2014**, *53*, 10021–10023.
[64] S. Aghazada, D. Fehn, F. W. Heinemann, D. Munz, K. Meyer, *Angew. Chem. Int. Ed.* **2021**, *60*, 11138–11142; *Angew. Chem.* **2021**, *133*, 11238–11242.
[65] S. Aghazada, M. Miehlich, J. Messelberger, F. W. Heinemann, D. Munz, K. Meyer, *Angew. Chem. Int. Ed.* **2019**, *58*, 18547–18551; *Angew. Chem.* **2021**, *131, 18719–18723*.
[66] a) F. W. B. Einstein, X. Yan, D. Sutton, *J. Chem. Soc. Chem. Commun.* **1990**, 1466–1467; b) K. D. Schramm, J. A. Ibers, *Inorg. Chem.* **1980**, *19*, 1231–1236.
[67] For a perspective on masked metallonitrene complexes of early transition metals, see: a) D. J. Mindiola, *Angew. Chem. Int. Ed.* **2008**, *47*, 1557–1559; for leading examples, see:; b) H. Herrmann, J. L. Fillol, H. Wadepohl, L. H. Gade, *Angew. Chem. Int. Ed.* **2007**, *46*, 8426–8430; c) J. D. Selby, C. D. Manley, M. Feliz, A. D. Schwarz, E. Clot, P. Mountford, *Chem. Commun.* **2007**, 4937–4939.
[68] a) G. Ferraudi, J. F. Endicott, *Inorg. Chem.* **1973**, *12*, 2389–2396; b) G.-Y. Gao, J. E. Jones, R. Vyas, J. D. Harden, X. P. Zhang, *J. Org. Chem.* **2006**, *71*, 6655–6658; c) V. Lyaskovskyy, A. I. O. Suarez, H. Lu, H. Jiang, X. P. Zhang, B. de Bruin, *J. Am. Chem. Soc.* **2011**, *133*, 12264–12273; d) K. H. Hopmann, A. Ghosh, *ACS Catal.* **2011**, *1*, 597–600; e) N. P. van Leest, M. A. Tepaske, B. Venderbosch, J.-P. H. Oudsen, M. Tromp, J. I. van der Vlugt, B. de Bruin, *ACS Catal.* **2020**, *10*, 7449–7463.
[69] M. Goswami, V. Lyaskovskyy, S. R. Domingos, W. J. Buma, S. Woutersen, O. Troeppner, I. Ivanović-Burmazović, H. Lu, X. Cui, X. P. Zhang, E. J. Reijerse, S. DeBeer, M. M. van Schooneveld, F. F. Pfaff, K. Ray, B. de Bruin, *J. Am. Chem. Soc.* **2015**, *137*, 5468–5479.
[70] M. G. Scheibel, J. Abbenseth, M. Kinauer, F. W. Heinemann, C. Würtele, B. de Bruin, S. Schneider, *Inorg. Chem.* **2015**, *54*, 9290–9302.
[71] J. E. Jones, J. V. Ruppel, G.-Y. Gao, T. M. Moore, X. P. Zhang, *J. Org. Chem.* **2008**, *73*, 7260–7265.
[72] L. Nurdin, D. M. Spasyuk, W. E. Piers, L. Maron, *Inorg. Chem.* **2017**, *56*, 4157–4168.
[73] A. A. Danopoulos, G. Wilkinson, T. K. N. Sweet, M. B. Hursthouse, *J. Chem. Soc. Dalton Trans.* **1996**, 3771–3778.
[74] K. Shin, H. Kim, S. Chang, *Acc. Chem. Res.* **2015**, *48*, 1040–1052.
[75] A. M. Geer, C. Tejel, J. A. Lopez, M. A. Ciriano, *Angew. Chem. Int. Ed.* **2014**, *53*, 5614–5618; *Angew. Chem.* **2014**, *126*, 5720-5724 .
[76] a) R. Breslow, S. H. Gellman, *J. Am. Chem. Soc.* **1983**, *105*, 6728–6729; b) I. Nägeli, C. Baud, G. Bernardinelli, Y. Jacquier, M. Moraon, P. Müller, *Helv. Chim. Acta.* **1997**, *80*, 1087–1105; c) X. Lin, C. Zhao, C.-M. Che, Z. Ke, D. L. Phillips, *Chem. Asian J.* **2007**, *2*, 1101–1108; d) M. Zenzola, R. Doran, R. Luisi, J. A. Bull, *J. Org. Chem.* **2015**, *80*, 6391–6399; e) C. G. Espino, J. Du Bois, *Angew. Chem. Int. Ed.* **2001**, *40*, 598–600; *Angew. Chem.* **2001**, *113*, 618–620; f) K. Hong, H. Su, C. Pei, X. Lv, W. Hu, L. Qiu, X. Xu, *Org. Lett.* **2019**, *21*, 3328–3331; g) M. P. Paudyal, A. M. Adebesin, S. R. Burt, D. H. Ess, Z. Ma, L. Kürti, J. R. Falck, *Science* **2016**, *353*, 1144; h) H. M. L. Davies, J. R. Manning, *Nature* **2008**, *451*, 417–424; i) Q. Nguyen, K. Sun, T. G. Driver, *J. Am. Chem. Soc.* **2012**, *134*, 7262–7265.
[77] R. H. Perry, T. J. Cahill, J. L. Roizen, J. Du Bois, R. N. Zare, *Proc. Nat. Acad. Sci.* **2012**, *109*, 18295–18299.
[78] a) J. F. Berry, *Dalton Trans.* **2012**, *41*, 700–713; b) J. Ciesielski, G. Dequirez, P. Retailleau, V. Gandon, P. Dauban, *Chem. Eur. J.* **2016**, *22*, 9338–9347; c) A. Varela-Álvarez, T. Yang, H. Jennings, K. P. Kornecki, S. N. Macmillan, K. M. Lancaster, J. B. C. Mack, J. Du Bois, J. F. Berry, D. G. Musaev, *J. Am. Chem. Soc.* **2016**, *138*, 2327–2341; d) E. Azek, C. Spitz, M. Ernzerhof, H. Lebel, *Adv. Synth. Catal.* **2020**, *362*, 384–397.
[79] A. Das, A. G. Maher, J. Telser, D. C. Powers, *J. Am. Chem. Soc.* **2018**, *140*, 10412–10415.
[80] A. Das, Y.-S. Chen, J. H. Reibenspies, D. C. Powers, *J. Am. Chem. Soc.* **2019**, *141*, 16232–16236.
[81] A. Das, C.-H. Wang, G. P. Van Trieste, C.-J. Sun, Y.-S. Chen, J. H. Reibenspies, D. C. Powers, *J. Am. Chem. Soc.* **2020**, *142*, 19862–19867.
[82] a) J. Ashley-Smith, M. Green, N. Mayne, F. G. A. Stone, *J. Chem. Soc. D: Chem. Commun.* **1969**, 409–409; b) B. C. Lane, J. W. McDonald, F. Basolo, R. G. Pearson, *J. Am. Chem. Soc.* **1972**, *94*, 3786–3793; c) H. W. Anderson, S. D. Clark, T. M. Ozretich, W. R. Moore, *J. Am. Chem. Soc.* **1971**, *22*, 4934–4935.
[83] D. S. Glueck, F. J. Hollander, R. G. Bergman, *J. Am. Chem. Soc.* **1989**, *111*, 2719–2721.
[84] D. S. Glueck, J. Wu, F. J. Hollander, R. G. Bergman, *J. Am. Chem. Soc.* **1991**, *113*, 2041–2054.
[85] J. Ryu, J. Kwak, K. Shin, D. Lee, S. Chang, *J. Am. Chem. Soc.* **2013**, *135*, 12861–12868.
[86] T. Kang, Y. Kim, D. Lee, Z. Wang, S. Chang, *J. Am. Chem. Soc.* **2014**, *136*, 4141–4144.
[87] C. L. Lee, L. Wu, J.-S. Huang, C.-M. Che, *Chem. Commun.* **2019**, *55*, 3606–3609.
[88] M. Kinauer, M. Diefenbach, H. Bamberger, S. Demeshko, E. J. Reijerse, C. Volkmann, C. Würtele, J. van Slageren, B. de Bruin, M. C. Holthausen, S. Schneider, *Chem. Sci.* **2018**, *9*, 4325–4332.
[89] M. G. Scheibel, B. Askevold, F. W. Heinemann, E. J. Reijerse, B. de Bruin, S. Schneider, *Nat. Chem.* **2012**, *4*, 552–558.
[90] a) R. Waterman, G. L. Hillhouse, *J. Am. Chem. Soc.* **2008**, *130*, 12628–12629; b) T. R. Cundari, J. O. C. Jimenez-Halla, G. R. Morello, S. Vaddadi, *J. Am. Chem. Soc.* **2008**, *130*, 13051–13058; c) V. M. Iluc, G. L. Hillhouse, *J. Am. Chem. Soc.* **2010**, *132*, 15148–15150; d) E. Kogut, H. L. Wiencko, L. Zhang, D. E. Cordeau, T. H. Warren, *J. Am. Chem. Soc.* **2005**, *127*,

11248–11249; e) D. J. Mindiola, G. L. Hillhouse, *Chem. Commun.* **2002**, 1840–1841.
[91] Y.-W. Ge, Y. Ye, P. R. Sharp, *J. Am. Chem. Soc.* **1994**, *116*, 8384–8385.
[92] Y. Dong, R. M. Clarke, G. J. Porter, T. A. Betley, *J. Am. Chem. Soc.* **2020**, *142*, 10996–11005.
[93] Y. Dong, C. J. Lund, G. J. Porter, R. M. Clarke, S.-L. Zheng, T. R. Cundari, T. A. Betley, *J. Am. Chem. Soc.* **2021**, *143*, 817–829.
[94] a) T. Migita, K. Hongoh, H. Naka, S. Nakaido, M. Kosugi, *Bull. Chem. Soc. Jpn.* **1988**, *61*, 931–938; b) E. J. Corey, J. O. Link, *J. Am. Chem. Soc.* **1992**, *114*, 1906–1908; c) D. L. Broere, B. de Bruin, J. N. Reek, M. Lutz, S. Dechert, J. I. van der Vlugt, *J. Am. Chem. Soc.* **2014**, *136*, 11574–11577; d) D. L. J. Broere, N. P. van Leest, B. de Bruin, M. A. Siegler, J. I. van der Vlugt, *Inorg. Chem.* **2016**, *55*, 8603–8611.
[95] a) A. Grünwald, D. Munz, *J. Organomet. Chem.* **2018**, *864*, 26–36; b) D. Munz, *Chem. Sci.* **2018**, *9*, 1155–1167.
[96] H.-Y. Thu, W.-Y. Yu, C.-M. Che, *J. Am. Chem. Soc.* **2006**, *128*, 9048–9049.
[97] S. J. Goodner, A. Grünwald, F. W. Heinemann, D. Munz, *Aust. J. Chem.* **2019**, *72*, 900–903.
[98] E. Poverenov, I. Efremenko, A. I. Frenkel, Y. Ben-David, L. J. W. Shimon, G. Leitus, L. Konstantinovski, J. M. L. Martin, D. Milstein, *Nature* **2008**, *455*, 1093–1096.
[99] A. W. Cook, P. Hrobárik, P. L. Damon, D. Najera, B. Horváth, G. Wu, T. W. Hayton, *Inorg. Chem.* **2019**, *58*, 15927–15935.
[100] a) Z. Li, R. W. Quan, E. N. Jacobsen, *J. Am. Chem. Soc.* **1995**, *117*, 5889–5890; b) S.-L. Abram, I. S. Monte-Pérez, F. F. Pfaff, E. R. F. and, K. Ray, *Chem. Commun.* **2014**, *50*, 9852–9854; c) F. Thomas, M. Oster, F. Schön, K. C. Göbgen, B. Amarouch, D. Steden, A. Hoffmann, S. Herres-Pawlis, *Dalton Trans.* **2021**, *50*, 6444–6462; d) J. Moegling, A. Hoffmann, F. Thomas, N. Orth, P. Liebhäuser, U. Herber, R. Rampmaier, J. Stanek, G. Fink, I. Ivanović-Burmazović, S. Herres-Pawlis, *Angew. Chem. Int. Ed.* **2018**, *57*, 9154–9159; *Angew. Chem.* **2018**, *130*, 9294–9299; e) L. Maestre, W. M. C. Sameera, M. M. Díaz-Requejo, F. Maseras, P. J. Pérez, *J. Am. Chem. Soc.* **2013**, *135*, 1338–1348; f) H. Kwart, A. A. Khan, *J. Am. Chem. Soc.* **1967**, *89*, 1951–1953; g) T. Corona, L. Ribas, M. Rovira, E. R. Farquhar, X. Ribas, K. Ray, A. Company, *Angew. Chem. Int. Ed.* **2016**, *55*, 14005–14008; *Angew. Chem.* **2016**, *128*, 14211–14214.
[101] F. Dielmann, O. Back, M. Henry-Ellinger, P. Jerabek, G. Frenking, G. Bertrand, *Science* **2012**, *337*, 1526–1528.
[102] A. G. Bakhoda, Q. Jiang, J. A. Bertke, T. R. Cundari, T. H. Warren, *Angew. Chem. Int. Ed.* **2017**, *56*, 6426–6430; *Angew. Chem.* **2017**, *129*, 6526–6530.
[103] M. J. B. Aguila, Y. M. Badiei, T. H. Warren, *J. Am. Chem. Soc.* **2013**, *135*, 9399–9406.
[104] A. (Gus) Bakhoda, Q. Jiang, Y. M. Badiei, J. A. Bertke, T. R. Cundari, T. H. Warren, *Angew. Chem. Int. Ed.* **2019**, *58*, 3421–3425; *Angew. Chem.* **2019**, *131*, 3459–3463.
[105] a) D. Schröder, H. Schwarz, *Angew. Chem. Int. Ed.* **1995**, *34*, 1973–1995; *Angew. Chem.* **1995**, *107*, 2126–2150; b) J. Roithová, D. Schröder, *Chem. Rev.* **2010**, *110*, 1170–1211; c) H. Schwarz, S. Shaik, J. Li, *J. Am. Chem. Soc.* **2017**, *139*, 17201–17212; d) N. Dietl, M. Schlangen, H. Schwarz, *Angew. Chem. Int. Ed.* **2012**, *51*, 5544–5555; *Angew. Chem.* **2012**, *124*, 5638-5650 .
[106] a) N. Dietl, C. van der Linde, M. Schlangen, M. K. Beyer, H. Schwarz, *Angew. Chem. Int. Ed.* **2011**, *50*, 4966–4969; *Angew. Chem.* **2011**, *123*, 5068–5072; b) E. Rezabal, J. Gauss, J. M. Matxain, R. Berger, M. Diefenbach, M. C. Holthausen, *J. Chem. Phys.* **2011**, *134*, 064304.
[107] M. Srnec, R. Navrátil, E. Andris, J. Jašík, J. Roithová, *Angew. Chem. Int. Ed.* **2018**, *57*, 17053–17057; *Angew. Chem.* **2018**, *130*, 17299–17303.
[108] S. Zhou, J. Li, M. Schlangen, H. Schwarz, *Angew. Chem. Int. Ed.* **2016**, *55*, 10877–10880; Angew. Chem. **2016**, 128, 11036–11039.
[109] a) N. J. Rijs, P. González-Navarrete, M. Schlangen, H. Schwarz, *J. Am. Chem. Soc.* **2016**, *138*, 3125–3135; b) L. Andrews, X. Wang, Y. Gong, T. Schlöder, S. Riedel, M. J. Franger, *Angew. Chem. Int. Ed.* **2012**, *51*, 8235–8238; *Angew. Chem.* **2012**, *124*, 8359–8363.
[110] L. Li, H. Beckers, T. Stüker, T. Lindič, T. Schlöder, D. Andrae, S. Riedel, *Inorg. Chem. Front.* **2021**, *8*, 1215–1228.
[111] M. W. Hussong, W. T. Hoffmeister, F. Rominger, B. F. Straub, *Angew. Chem. Int. Ed.* **2015**, *54*, 10331–10335; *Angew. Chem.* **2015**, *127*, 10472–10476.
[112] Y. Gong, L. Andrews, *Inorg. Chem.* **2012**, *51*, 667–673.
[113] K. Dehnicke, J. Straehle, *Chem. Rev.* **1993**, *93*, 981–994.
[114] T. Stüker, T. Hohmann, H. Beckers, S. Riedel, *Angew. Chem. Int. Ed.* **2020**, *59*, 23174–23179; *Angew. Chem.* **2020**, *132*, 23374–23379.
[115] a) B. M. Wolf, R. Anwander, *Chem. Eur. J.* **2019**, *25*, 8190–8202; b) D. Schadle, R. Anwander, *Chem. Soc. Rev.* **2019**, *48*, 5752–5805; c) C. Weetman, *Chem. Eur. J.* **2021**, *27*, 1941–1954; d) R. C. Fischer, P. P. Power, *Chem. Rev.* **2010**, *110*, 3877–3923; e) P. P. Power, *Chem. Rev.* **1999**, *99*, 3463–3504.

Manuscript received: May 13, 2021
Revised manuscript received: July 26, 2021
Accepted manuscript online: July 28, 2021